ELSEVIER

Contents lists available at ScienceDirect

Desalination

journal homepage: www.elsevier.com/locate/desal





Membrane-based indirect power generation technologies for harvesting salinity gradient energy - A review

Yanmei Jiao ^{a,1}, Linhui Song ^{a,1}, Cunlu Zhao ^b, Yi An ^a, Weiyu Lu ^a, Bin He ^{c,*}, Chun Yang ^{d,*}

- a School of Physical and Mathematical Sciences, Nanjing Tech University, Nanjing, PR China
- b Key Laboratory of Thermo-Fluid Science and Engineering of MOE, Xi'an Jiaotong University, Xi'an, PR China
- ^c School of Energy and Power Engineering, Nanjing university of science and technology, Nanjing, PR China
- ^d School of Mechanical and Aerospace Engineering, Nanyang Technological University, Singapore

HIGHLIGHTS

- Utilizing hypersaline sources as draw solution shows great potential.
- Integration with certain industrial processes provides mutual benefits.
- Further exploration of superior semipermeable membranes is urgently demanded.
- Improvement strategies for the osmosis and electric submodules are identified.

ARTICLE INFO

Keywords: Osmosis Salinity gradient energy Power generation Pressure retarded osmosis Electrokinetics Desalination

ABSTRACT

The giant and sustainable salinity gradient energy broadly occurs when mixing solution sources with different concentrations can be potentially harvested through the intensively studied membrane-based indirect power generation technologies. This kind of technology commonly has two functional submodules, namely the osmosis submodule to induce driven forces and the electric submodule to produce electricity. However, almost all relevant reviews only concentrate on the traditional pressure retarded osmosis (PRO) technology without involving newly emerged ones such as the forward osmosis-electrokinetic (FO-EK) technology, leading to outdated and incomplete knowledge in this field. Therefore, this study is going to provide a comprehensive and up-to-date review of the membrane-based indirect power generation technologies through adequately outlining most related research. The authors not only provide a systematic overview of the theoretical background and the development of the state-of-the-art membrane-based indirect power generation technologies but also highlight their essential characterizations. Meanwhile, the challenges and the optimizing strategies in aspects of efficient semipermeable membranes, available fluid materials, and operation conditions, as well as future promising applications in different scenarios are also elaborated in detail.

1. Introduction

Nowadays, the need for alternative green energy to realize carbon neutrality has long been a hot issue and becomes even more critical due to the deterioration in the environment and the depletion of the traditional fossil energy resources. Salinity gradient energy, commonly occurring when mixing solution sources with different concentrations, such as desalination brine, seawater, natural hypersaline source, and river water, is one of the widely studied green energies due to its vast

amount and promising sustainability [1–3]. Various technologies have been developed on a bench-scale or on a large scale to harvest this energy, including conventional technologies, such as pressure retarded osmosis (PRO) [4–6], reverse electrodialysis (RED) [7–9], and vapor pressure difference [10], and emerging technologies such as electric double-layer capacitor [11,12], faradaic pseudo-capacitor [13,14], forward osmosis-electrokinetic (FO-EK) [15], diffusio-osmosis [16], and nanofluidic reverse electrodialysis [17–19].

When a semipermeable membrane is used to separate two solutions

E-mail addresses: hebin@njust.edu.cn (B. He), MCYang@ntu.edu.sg (C. Yang).

^{*} Corresponding authors.

 $^{^{1}}$ These authors contribute equally.

with different salinity, a spontaneous oriented transport of solvent occurs, which is commonly called as osmosis process [20]. The difference in solution salinity between those two solutions leads to a chemical potential difference, in other words, the osmotic pressure difference, which in essence is the driving force for the movement of the solvent molecules from the solution with low concentration to that with high concentration. In fact, the mathematical expression of the osmotic pressure does not depend on the nature of the solute or that of the membrane. The concentration and the stoichiometric numbers of the anion and the cation are the only parameters that affect the osmotic pressure. In this sense, a process can be called an osmosis one as long as there are movements of the solvent and the solute driven by the osmotic pressure difference, no matter whether there is a semipermeable membrane or not [21]. In terms of the simultaneity of the power generation process with the osmosis process, the aforementioned power generation technologies can be classified into three main categories. The first category is membrane-based indirect technology, including the PRO and the FO-EK technologies, the power generation process and the osmosis process of which occur within different functional submodules. The osmosis process occurring in the osmosis submodule induces mechanical movement of the solution, which is utilized in the electric submodule to drive the power generation process. The second category is the membrane-based direct technology, including the RED, the nanofluidic reverse electrodialysis, the electric double-layer capacitor, the faradaic pseudo-capacitor, and the diffusio-osmosis technologies, the power generation process and the osmosis process of which occur synchronously within the same functional unit. The osmosis process not only induces the movement of the solvent and the solute but also converts the movement of ions into electric current and/or electric potential simultaneously. The third category includes other power generation technologies, such as the vapor pressure difference technology. These technologies utilize other properties other than the osmotic property, such as the different evaporation rates of electrolyte solutions with different concentrations, to produce electricity indirectly.

The membrane-based indirect power generation technologies are the most widely studied and have great potential for producing energy in different applications. However, almost all current reviews only focus on the PRO without involving newly emerged technologies, leading to outdated and incomplete knowledge in this field [22-27]. In addition, the limitations, the challenges, and the corresponding promising solutions to current problems of the membrane-based indirect power generation technologies are not systematically studied yet. Therefore, this paper aims to provide a rounded and up-to-date review of both the traditional PRO technology and the newly developed FO-EK technology. The essential common features of the membrane-based indirect power generation technologies are newly extracted after investigating the related early works in this field. The authors not only offer state-of-theart development of the membrane-based indirect power generation technologies but also highlight their essential characterizations. Meanwhile, the challenges and the optimizing strategies, as well as future development, are also outlined in detail.

2. Theoretical background of osmosis and power generation

2.1. The Gibbs energy of mixing

The solution with a certain electrolyte concentration possesses a particular chemical potential, which can be quantitatively defined by the Gibbs energy G:

$$G = \sum_{i} C_{i}V(\mu_{i}^{0} + \nu_{i}\Delta p + |z_{i}|F\Delta\psi + RT\ln\gamma_{i}x_{i})$$
 (1)

where the subscript i represents the i-th component in the solution; C, V, ν , Δp , z, F, $\Delta \psi$, R, T, γ , and x, are the mole concentration, the total volume, the partial molar volume, the pressure difference, the valence,

the Faraday constant 96,485 C/mol, the electrical potential difference, the gas constant 8.314 J/mol/k, the solution temperature, the activity coefficient, and the mole fraction, respectively. Then the Gibbs energy released from the mixing of two solutions, ΔG_{mix} , is calculated as the difference between the overall Gibbs energy of the solutions before and after mixing and is given as:

$$\Delta G_{\text{mix}} = G_b - (G_c + G_d) \tag{2}$$

where subscripts b, c, and d represent the brackish solution, the concentrated solution, and the dilute solution, respectively. The analysis shows that the theoretically available amount of the Gibbs energy from mixing different natural solutions varies from 420 kJ in the case of mixing 1 m³ seawater (appr. 0.5 M NaCl) with 1 m³ reverse osmosis brine (appr. 1 M NaCl) to 16.8×10^3 kJ in the case of mixing 1 m³ river water (appr. 0.01 M NaCl) with 1 m³ reverse osmosis brine (appr. 5 M NaCl) [28].

However, the Gibbs energy released from the mixing of two solutions represented by Eq. (2) was developed under the assumption of reversibility that can be achieved if the osmosis process is operated in a batch mode and the applied pressure is infinitesimally smaller [6]. In real applications, the irreversibilities commonly occur in terms of friction losses from the pre-treatment of solutions, pumping systems, circulations of solutions, hydro-turbines, and pressure exchangers [29]. In addition, the non-ideal membranes are also a source of irreversibility [6].

2.2. Osmotic pressure

The osmotic pressure π of a solution with the concentration of C is given by Eq. (3), which was derived based on the theory of chemical equilibrium with two main assumptions: (1) the solution of a single solute is separated from the corresponding pure solvent by a semi-permeable membrane; (2) the osmosis system is in its equilibrium state. Parameters χ and β in the osmotic pressure equation are the osmotic coefficient and the stoichiometric number, respectively, and subscripts a and c represent the anion and the cation, respectively [30]. This equation shows that the osmotic pressure linearly decreases with the increasing solution concentration.

$$\pi = -\chi RT(\beta_a + \beta_c)C \tag{3}$$

2.3. Solvent permeating flux

Practically, extra pressures are usually induced or applied along with the pure osmosis process. Therefore, the solvent permeating flux, J_w , is then given by [31,32]:

$$J_w = A(\Delta \pi - \Delta P) \tag{4}$$

where A is the intrinsic water permeability coefficient of the membrane; $\Delta \pi$ is the osmotic pressure difference defined as $\pi_{CL} - \pi_{CH}$; ΔP is the extra pressure difference defined as $P_{CH} - P_{CL}$. The subscripts C_L and C_H represent solutions with low concentration and high concentration, respectively. According to the relationships between $\Delta \pi$ and ΔP , three typical osmosis statuses, including the forward osmosis (FO), the pressure retarded osmosis (PRO), and the reverse osmosis (RO), are determined, as shown in Fig. 1 [33].

As for FO, there is no pressure difference between P_{CH} and P_{CL} along with the pure osmosis process, in other words, $\Delta P=0$, and thus the solvent permeates from the low-concentration side to the high-concentration side without any extra resistance. As for PRO, although the pressure applied on the high-concentration side is higher than that applied on the low-concentration side, ΔP is still smaller than $\Delta \pi$. Therefore, the permeating direction of the solvent in the PRO process is the same as that in the FO process. As for RO, the pressure applied on the high-concentration side is much higher than that applied on the low-

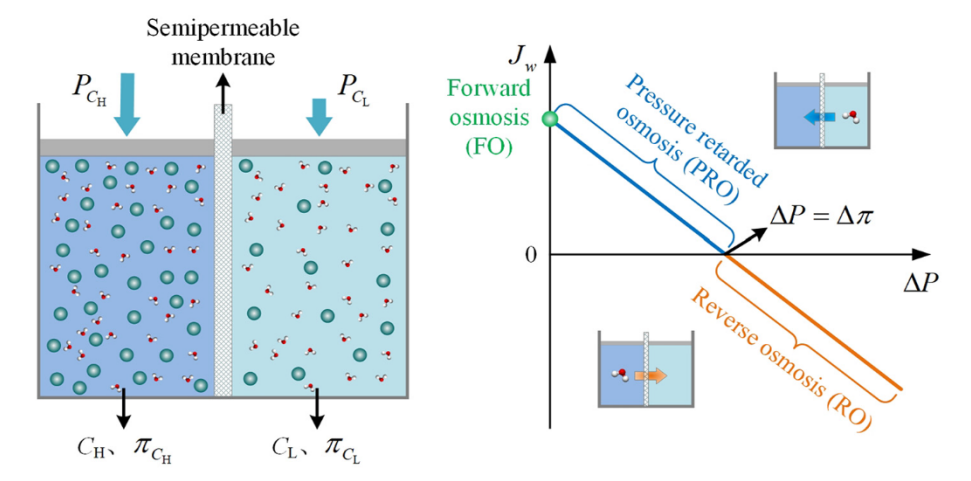


Fig. 1. Schematic of three typical osmosis statuses, including the forward osmosis (FO), the pressure retarded osmosis (PRO), and the reverse osmosis (RO). They are determined in light of the relationships between $\Delta \pi$ and ΔP ($\Delta \pi = \pi_{C_L} - \pi_{C_R}$ and $\Delta P = P_{C_R} - P_{C_L}$).

concentration side so that ΔP is larger than $\Delta \pi$ and the permeating direction of the solvent is from the high-concentration side to the low-concentration side. As a rule of thumb, the solution where the solvent permeates from/into along with the osmosis processes is termed as the feed solution (FS)/the draw solution (DS), respectively. Generally, FO and PRO are commonly applied in the field of power generation, while RO is widely employed in the field of water desalination.

2.4. Fouling, scaling, and concentration polarization

The performance of osmosis processes is commonly degraded by three phenomena, namely fouling, scaling, and concentration polarization (CP) [34]. Generally, the first two phenomena occur on or within the membrane, and the last one occurs in the region adjacent to the membrane within the solution. The membrane fouling is caused by the accumulation of suspending organic matters onto the surface or into the inner structure of the membrane [35–39]. The membrane scaling results from the precipitation of inorganic minerals, such as calcium, magnesium, barium, bicarbonate, and sulfate, and/or deposition of colloidal particles onto the membrane [40,41]. Both fouling and scaling lead to the degradation of the solvent permeating flux in osmosis processes and dramatically shorten the average lifetime of the membranes [42]. In addition, the status of fouling and scaling layers in FO and PRO processes are considerably different from that in RO processes because of the different pressure environments and permeating directions of the solvent. Chemical methods are often used to remove the membrane fouling and scaling to regain the solvent permeating flux in the RO processes, while mechanical methods such as increasing the velocity of

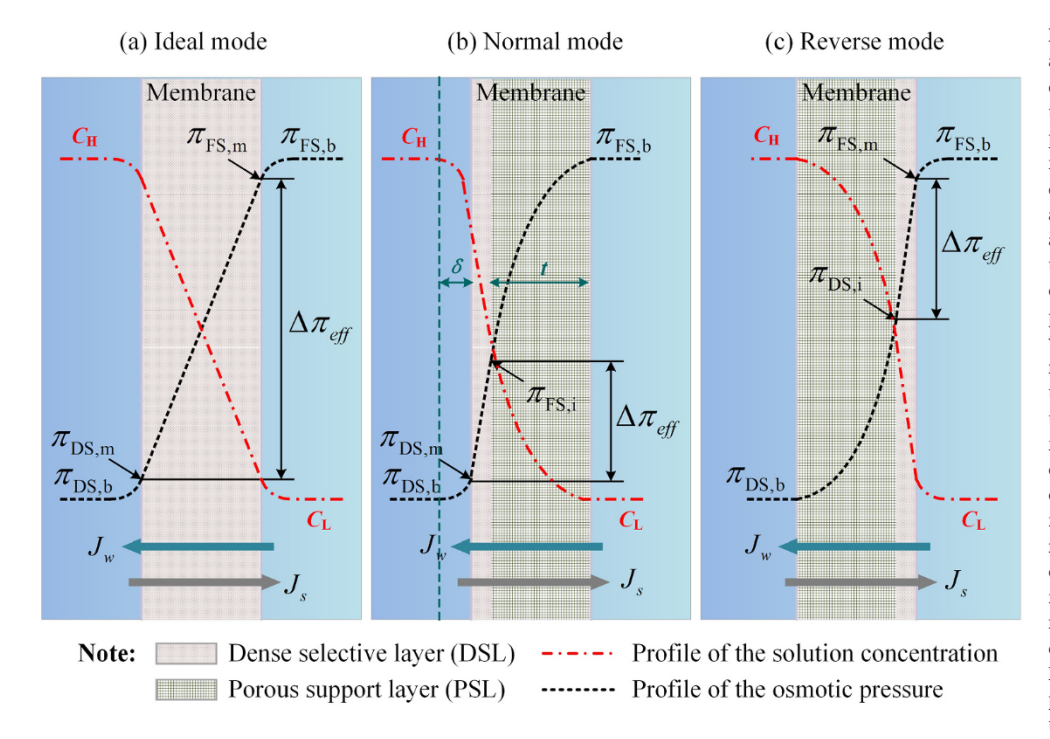


Fig. 2. Profiles of the solution concentration and the corresponding osmotic pressure for different membrane structures and orientations. (a) An ideal symmetric dense semipermeable membrane with only ECP, including the concentrative ECP and the dilutive ECP. (b) A practically applied asymmetric membrane with the DSL facing against the DS (Normal mode). The profile of solution concentration illustrates concentrative ICP and dilutive ECP. (c) A practically applied asymmetric membrane with the PSL facing against the DS (Reverse mode). The profile of the solution concentration illustrates dilutive ICP and concentrative ECP. Key parameters: CH and CL respectively represent solutions of high concentration and low concentration; $\pi_{DS,b}$ is the osmotic pressure in the bulk of the DS; $\pi_{DS,m}$ is the osmotic pressure in the vicinity of membrane surface at the DS side; $\pi_{FS,b}$ is the osmotic pressure in the bulk of the FS; $\pi_{FS,m}$ is the osmotic pressure in the vicinity of membrane surface at the FS side; $\pi_{FS,i}$ is the effective osmotic pressure of the FS in Normal mode; $\pi_{DS,i}$ is the effective osmotic pressure of the DS in Reverse mode; $\Delta \pi_{eff}$ is the effective osmotic pressure difference; J_w and J_s respectively are the solvent permeating flux and the reverse salt flux; δ is the distance between the DSL and the nearest

layer with the concentration of the bulk of DS; t is the thickness of the PSL. Note that it is assumed that no ECP occurs around the interface between the PSL and the solution since the solute is not reflected by this layer.

crossflow are often applied to achieve the similar goal in FO and PRO processes.

As for the CP, take the FO process shown in Fig. 2 as an example. Although CP happens within the solution, it is strongly related to the asymmetric structure of the practically applied semipermeable membrane, which consists of a thin dense selective layer (DSL) supported by a thick porous support layer (PSL). Both the solute and the solvent molecules can freely pass through the PSL, but only the small solvent molecules can pass through the DSL. Therefore, CP in the osmosis processes is classified into two categories, including the external concentration polarization (ECP) that occurs adjacent to the membrane and the internal concentration polarization (ICP) that occurs inside the PSL of the membrane [43–48].

Practically, unlike the fouling and the scaling that are periodic and can be regularly removed with chemical methods, the CP occurs as long as the osmosis process runs. Therefore, only the CP is considered when figuring out the permeating flux of the osmosis process. Since high extra pressures are usually applied onto the RO system, the effect of ICP on the RO performance, compared to the overwhelming effect of ECP, is relatively small and thus can be ignored. However, for the solvent permeating flux in FO and PRO processes, both ICP and ECP effects should be considered in the theoretical mode [49]. Moreover, different orientations of the asymmetric membrane give rise to different types of ICP/ ECP. When the DSL of the membrane faces against the DS (Normal mode), as shown in Fig. 2.b, the solute is enriched within the PSL but diluted nearby the DSL at the DS side, leading to the concentrative ICP and the dilutive ECP. On the contrary, when the PSL faces against the DS (Reverse mode), as shown in Fig. 2.c, the solute is enriched nearby the DSL at the FS side and diluted within the PSL, leading to the concentrative ECP and the dilutive ICP. The presence of CP degrades the performance of the osmosis process due to the reduced effective osmotic pressure difference between the FS and the DS. In real applications, the Normal mode is the most frequently employed running mode since the CP phenomenon in this mode is less significant than that in the Reverse mode. The corresponding solvent permeating flux J_w for FO/PRO in the Normal mode is given as:

$$J_{w} = A \left\{ \frac{\pi_{\text{FS,b}} exp\left(\frac{J_{w}S}{D}\right) - \pi_{\text{DS,b}} exp\left(-\frac{J_{w}}{k}\right)}{1 + \frac{B}{J_{w}} \left[exp\left(\frac{J_{w}S}{D}\right) - exp\left(-\frac{J_{w}}{k}\right) \right]} - \Delta P \right\}$$
(5)

where the subscript b represents the bulk region of the corresponding FS/DS; $k=D/\delta$ is the mass transfer coefficient within the dilutive ECP layer with D and δ respectively being the solute diffusion coefficient and the distance between the DSL and the nearest layer with the concentration of the bulk of DS; S denotes a structure factor related to the PSL and is defined as $S=t\tau/\theta$ with t,τ , and θ respectively representing the thickness, the tortuosity, and the porosity of the PSL; B is the salt permeability coefficient of the DSL of the membrane [50].

2.5. Reverse salt flux

Ideally, the semipermeable membrane should completely reject the solute molecules transporting from the high-concentration side to the low-concentration side. However, in practical applications, the solutes unavoidably diffuse through the semipermeable membrane due to the non-ideal characteristic of the semipermeable membrane. This characteristic can be reflected by a parameter called solute rejection, $R_j=1-C_p/C_{\rm FS}$, where C_p is the solute concentration of the permeate solution obtained in the corresponding RO experiments and $C_{\rm FS}$ is that of the FS, and the overall term $C_p/C_{\rm FS}$ denotes the solute passage. Then the permeability coefficient of the DSL of membrane B mentioned above can be determined from [51]:

$$B = J_w \left(\frac{1 - R_j}{R_i} \right) exp \left(-\frac{J_w}{k_f} \right)$$
 (6)

where $k_{\rm f}$ is the crossflow cell mass transfer coefficient. In addition, another important parameter indirectly reflecting the intrinsic non-ideal property of the semipermeable membrane is the reverse salt flux which can be expressed as a function of J_w [50,52]:

$$J_{s} = B \left\{ \frac{C_{\text{DS,b}} exp\left(-\frac{J_{w}}{k}\right) - C_{\text{FS,b}} exp\left(\frac{J_{w}S}{D}\right)}{1 + \frac{B}{J_{w}} \left[exp\left(\frac{J_{w}S}{D}\right) - exp\left(-\frac{J_{w}}{k}\right)\right]} \right\}$$
(7)

The salt leaking from the DS side to the FS side greatly reduces the effective osmotic pressure difference between the solutions beside the membrane and thus weakens the solvent flux.

2.6. Energy conversion performance

2.6.1. PRO technology

Loeb et al. conducted a preliminary study in 1976 on the PRO power generation from salinity gradient energy. Fig. 3 shows the schematic of a continuous power generation system based on the PRO technology. The asymmetric Du Pont Permasep B-10 hollow-fibers enclosed in minipermeators in the form of a U-shape were utilized as the semipermeable membrane. The feed brine was pressurized and filtered outside the hollow fibers while the water permeated into the inside space. The continuous permeation of water from the water side to the brine side because of the osmotic pressure difference increased the potential energy of the brine solution, thereby driving the hydroturbine and the generator to generate electricity. Part of the generated electricity was used to power the water pump and the recycle pump, and the remnant was merged into the busbar. Their study also estimated that an economic benefit of 0.07 USD/kW/h could be achieved by a PRO power generation system with Dead Sea brine and water being respectively utilized as the DS and the FS. This system, however, has several drawbacks, including low efficiency of rotating components, friction losses in plant streams, and imperfect semipermeable membranes [4,53].

In the PRO power generation process, the power density is defined as the generated power per unit membrane area and is expressed by the water permeating flux and the hydraulic pressure difference across the membrane:

$$W_{\rm PRO} = J_{\rm w} \Delta P \tag{8}$$

Since the general expression for the permeating flux is $J_w = A(\Delta \pi_{eff} - \Delta P)$, the theoretical maximum power density occurs when $\Delta P = \Delta \pi_{eff}/2$, as schematized in Fig. 4.

The maximum power density is derived as [31,54]:

$$W_{\text{PRO},max} = A \frac{\Delta \pi_{\text{eff}}^2}{4} \tag{9}$$

Some typical laboratory studies on the PRO power generation performance utilizing different membranes and DS/FS pairs are selectively summarized in Table 1 in chronological order. It is worth noting that this commonly utilized expression of the power density is indirectly derived from the performance of the osmosis processes. Thus, it is only an ideal estimation and cannot truly reflect the effects of each power generation component.

2.6.2. FO-EK technology

As aforementioned, FO can provide considerable driving forces for fluid movement. Hon et al. and Jiao et al. proposed a novel FO-EK power generation system, as shown in Fig. 5, to harvest the salinity energy by applying the FO mechanism [15,65]. As implied by the name, the hybrid FO-EK power generation system is mainly composed of two submodules, namely the FO submodule and the EK submodule, as shown in Fig. 5.a.

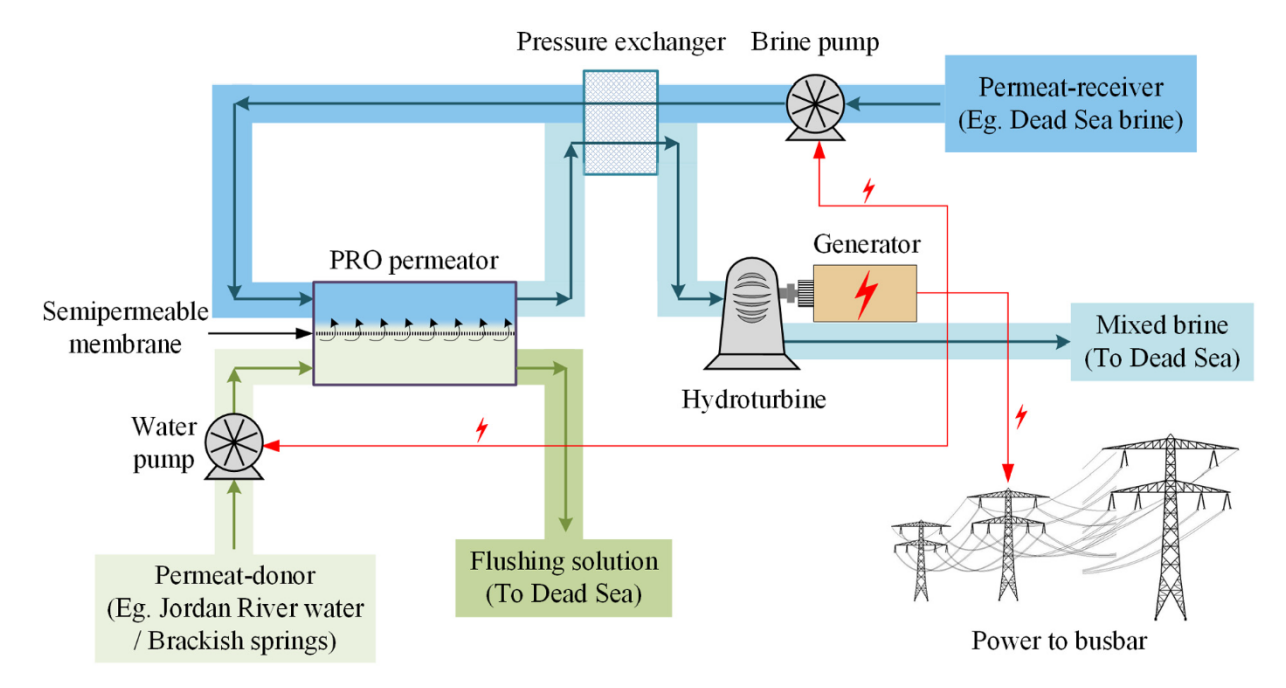


Fig. 3. Schematic of the pressure retarded osmosis (PRO) power generation plant located in the Dead Sea (adapted with permission from Ref. [53]).

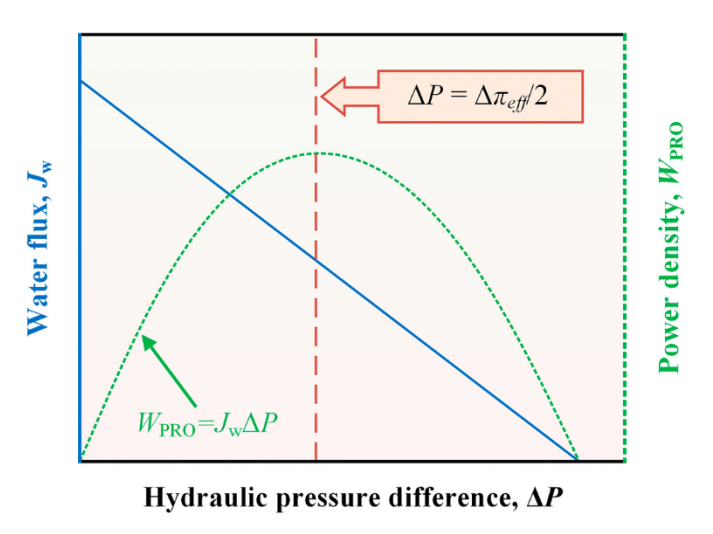


Fig. 4. The relationships among the water permeating flux, the hydraulic pressure difference, and the power density.

The former induces continuous transportation of fluid passing through the whole system, and the latter mainly focuses on generating electricity. A porous glass is sealed within the EK submodule, as shown in Fig. 5.b. It is the functional element for electricity generation through the mechanism of the pressure-driven EK flows. The emerging FO-EK technology is thoroughly investigated from the viewpoint of the complete power generation system, which not only includes the osmosis components but also includes the power generation components.

As known, the EK process is an interfacial phenomenon commonly occurring at the interface of the majority of objects. Taking the porous glass as an example, once it contacts an electrolyte solution, its surface is negatively charged due to the dissociation of the silanol group. Thus, it attracts cations and repels anions in the electrolyte solution, leading to an electric double layer (EDL) adjacent to the intersurface, as shown in Fig. 5.c. The corresponding EDL thickness λ is expressed as $\lambda = (\varepsilon_0 \varepsilon_1 k_B T)^{1/2}/(\Sigma e^2 z_k^2 n_{k,\infty})^{1/2}$ with the subscript k denoting the kth ion [66,67]. Therefore, the electrolyte solution within the microchannel exhibits an overall electric property of being positively charged. When

the electrolyte solution is continuously driven to pass through the porous glass, a streaming current I_s is generated by the forward convection flow. At the same time, a streaming potential E_x is also induced by the accumulation of the cations at the down streaming end, which conforms to the principle of electrostatics. The streaming potential E_x , in turn, induces a conduction current I_c through the bulk electrolyte solution. The streaming potential and the streaming current can be properly harvested as a kind of power source when the two ends of the micro/nano-channel are connected by an external electric circuit.

The streaming current and the streaming potential have been thoroughly studied for several decades [68–70]. According to previous studies, an extra pump is required to drive the FS through the porous glass to generate electricity. However, the novel FO-EK power generation system alternatively utilizes an FO submodule to induce a convection flow of the FS. The electric energy is successively produced within the EK submodule. Similar to the PRO system, the only energy input of the FO-EK system comes from the pump and is used to circulate and refresh the DS throughout the FO submodule to maintain the osmotic pressure difference between the two sides of the semipermeable membrane and thus to maintain the continuous power generation for the whole system. However, the energy consumed by the circulation pump is significantly smaller than that consumed by the traditional pressure-driven EK process.

Theoretically, in addition to the solvent permeating flux for the FO process (Eq. (3)), the mathematical model of the streaming potential and the streaming current should also be involved in the overall mathematical model of the FO-EK power generation system. It mainly includes governing equations of the Poisson-Boltzmann (P-B) equation (Eq. (10)) for describing electric potential profile in the EDL and the Navier-Stokes (N-S) equation (Eq. (11)) and the continuity equation (Eq. (12)) for describing the fluid flow field [71]. In addition, the Nernst-Planck (N-P) equation (Eq. (13)) is employed to describe the ion transport in micro/nano-channels.

$$\nabla^2 \psi = \frac{1}{\lambda^2} \psi \tag{10}$$

$$\rho \mathbf{u} \cdot \nabla \mathbf{u} = \nabla \mathbf{P} + \mu \nabla^2 \mathbf{u} + \rho_e \mathbf{E}$$
(11)

$$\nabla \cdot \mathbf{u} = 0 \tag{12}$$

Table 1A selective review of the studies on the power generation performance of PRO.

Case	Feed solution	Draw solution	Pressure, MPa	Membrane	Power density, W/m^2
Loeb et al., 1976 [53]	Filtered and distilled water	Dead Sea brine	1.2	Asymmetric Du Pont Permasep B-10 hollow fibers	0.35
Jellinek and Masuda, 1981 [55]	Fresh water	0.612 M NaCl solution	1.395	CTA membrane	1.6
Gerstandt et al., 2008 [56]	Fresh water	35 g/L NaCl solution	1.45	TFC hollow fiber membrane	3.5
Achilli et al., 2009 [57]	DI water	35 g/L NaCl solution 60 g/L NaCl solution	0.97	CTA flat-sheet membrane	2.7 5.1
Yip et al., 2011 [50]	River water	Seawater	1.25	TFC membrane	10
Chou et al., 2012 [58]	River water (10 mM NaCl)	Seawater (0.5 M NaCl)	0.5	TFC hollow fiber membrane	5.7
Gnou et al., 2012 [30]	Wastewater brine (40 mM NaCl)	beawater (old in Hadi)	0.49	II d nonow liber membrane	3.3
	Wastewater Sime (10 mm Hadi)		0.89		5,6
	Concentrated wastewater brine (80		0.47		2.8
	mM NaCl)		0.89		4.1
	River water (10 mM NaCl)	Seawater brine (1.0 M	0.84		11
	Wastewater brine (40 mM NaCl)	NaCl)	0.51		6.2
			0.9		10.6
	Concentrated wastewater brine (80		0.5		4.7
	mM NaCl)		0.91		8.4
Kim et al., 2013 [59]	Tap water	0.6 M NaCl solution	0.98	Spiral-Wound PRO Membrane	1
Li and Chung, 2014 [60]	Fresh water	1 M NaCl solution	2.1	TFC P84 co-polyimide hollow fiber 12 membrane	
Higa et al., 2017 [61]	Tap water	0.5 M NaCl solution	0.8	CTA hollow fiber membrane	0.14
Li et al., 2017 [62]	DI water with foulant of 200 ppm alginate	1 M NaCl solution	1.5	Modified TFC hollow fiber membrane	16.2
Sharma et al., 2019 [63]	DI water	0.6 M NaCl solution	/	Modified CA flat membranes	3.1
Moon et al., 2020 [64]	DI water	1 M NaCl solution	2.1	Chlorine-treated TFC membrane	26.6

CTA: Cellulose triacetate. CA: Cellulose acetate. TFC: Thin-film composites.

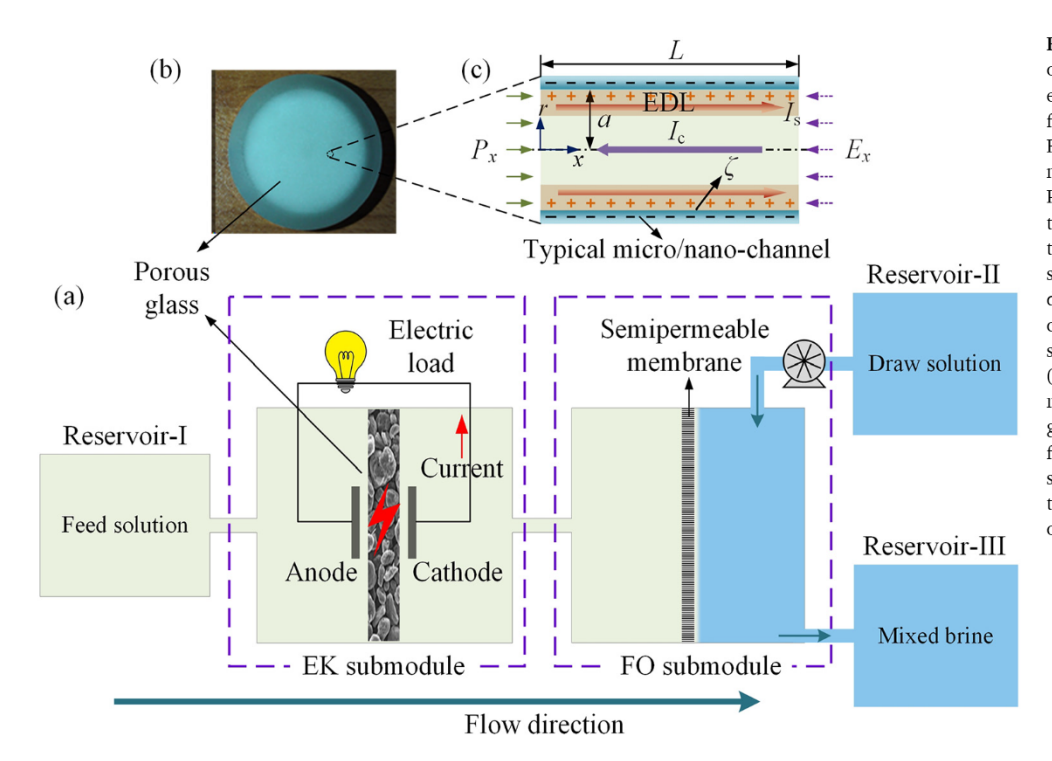


Fig. 5. (a) Schematic of the forward osmosis-electrokinetic (FO-EK) power generation system (adapted with permission from Ref. [15]). (b) Porous glass used in the FO-EK power generation system to provide micro/nano-channels for the EK flow. (c) Pressure-driven EK flow passing through a typical equivalent micro/nano-channel of the porous glass. The micro/nano-channel surface is negatively charged due to the dissociation of silanol groups, which attracts cations and repels anions in the electrolyte solution, inducing an electric double layer (EDL) adjacent to the intersurface. P_x and E_x respectively represent the applied pressure gradient, dP/dx, and the induced electric field strength, $\partial \phi / \partial x$; I_s , I_c , a, L, and ζ are the streaming current, the conduction current, the radius, the length, and the zeta potential of the micro/nano-channel, respectively.

$$\Gamma_{\mathbf{k}} = -\frac{ez_{\mathbf{k}}D_{\mathbf{k}}}{k_{\mathbf{p}}T}n_{\mathbf{k}}\nabla\psi + n_{\mathbf{k}}\mathbf{u}$$
(13)

where ψ denotes the static electric potential, e the absolute value of proton charge, \mathbf{u} the fluid velocity, ρ the fluid density, μ the fluid viscosity, ρ_e the charge density, \mathbf{E} the electric field strength, Γ the ionic flux, D the diffusivity of the ion, n ionic number concentration.

Initially, Hon et al. treated the porous glass as a bundle of micro/nano-channels with a uniform radius and developed a semi-empirical mathematical model for the FO-EK power generation system. Realizing the strong dependence of the energy conversion performance on the channel radius [72,73], Jiao et al. refined the aforementioned mathematical model with an assumption that the radii of the equivalent micro/nano-channels of the porous glass follow a log-normal probability

density distribution. The refined model yields much more consistent results with the experimental results [15]. In addition, as a key parameter in evaluating the energy conversion performance of the FO-EK system, the power density is defined as the ratio of the generated power to the effective volume of the porous glass. Since it is assumed that the streaming current linearly decreases with the increment of the streaming potential, the maximum power density occurs at half of the streaming potential [68,70] and can be derived as follow:

$$W_{\rm FO-EK,max} = \frac{1}{4} \frac{\Delta \phi I_s}{V_{eff}} \tag{14}$$

where $\Delta\phi$ and I_s are the streaming potential and the streaming current, respectively, and V_{eff} is the effective volume of the porous glass used in the EK submodule. Jiao et al. demonstrated that the experimental and the corresponding theoretical maximum power densities were achieved as 0.165 W/m³ and 0.241 W/m³, respectively, when the average pore size of the porous glass is 6 μ m and the salinity difference between the FS and the DS is 4 M [15]. Accordingly, an estimated economic cost of 0.069 USD/kW/h can be obtained based on the assumed service life of 10 years of the porous glass, which is comparable to the one of PRO technology.

In addition to the refinement of the theoretical model of the FO-EK system, the test of methodologies applied to enhance the pressure-driven EK flow through the porous glass, such as surface treatments, were also conducted. It is reported that both the large hydrophobic interface and the high surface charge density of the micro/nano-channels, which contribute to a faster liquid flow and a higher zeta potential, respectively, can significantly enhance the energy conversion performance of the EK flows [74–77]. Therefore, Jiao et al. applied the

ultrasonic physical treatment and the sodium dodecyl sulfate (SDS) surfactant treatment (with SDS concentration of 12 mM) on the porous glass to enhance the energy conversion performance. A maximum power density of 3.08 W/m^3 was obtained, around 30% higher than that obtained from the untreated porous glass [78].

3. Developments and challenges

3.1. The osmosis submodule

3.1.1. The efficiency of the membrane

The efficiency of the semipermeable membrane is always the most concerned issue in developing membrane-based power generation systems on a large scale. According to the review, thin-film composites (TFC) hollow fiber membrane [50,58,60,62,79–85] and asymmetric cellulose triacetate/cellulose acetate (CTA/CA) flat-sheet membrane [63,86–88], as shown in Fig. 6 and Fig. 7 respectively, are the most commonly studied membranes in both academic and industrial applications.

Different structures of the semipermeable membrane give rise to different membrane properties, including porosity, mass transfer efficiency, semipermeability, fouling, scaling, and CP. Gerstandt et al. conducted an overall performance evaluation on TFC hollow fiber membrane and asymmetric CTA/CA flat-sheet membrane from the aspect of power generation and found that power densities obtained by PRO were only 3.5 W/m² and 1.3 W/m², respectively [56], and the power densities achieved by the FO-EK are only in the order of 10^{-6} W/m² [15]. The power density should be at least larger than 4 W/m² for a promising and profitable membrane-based energy conversion

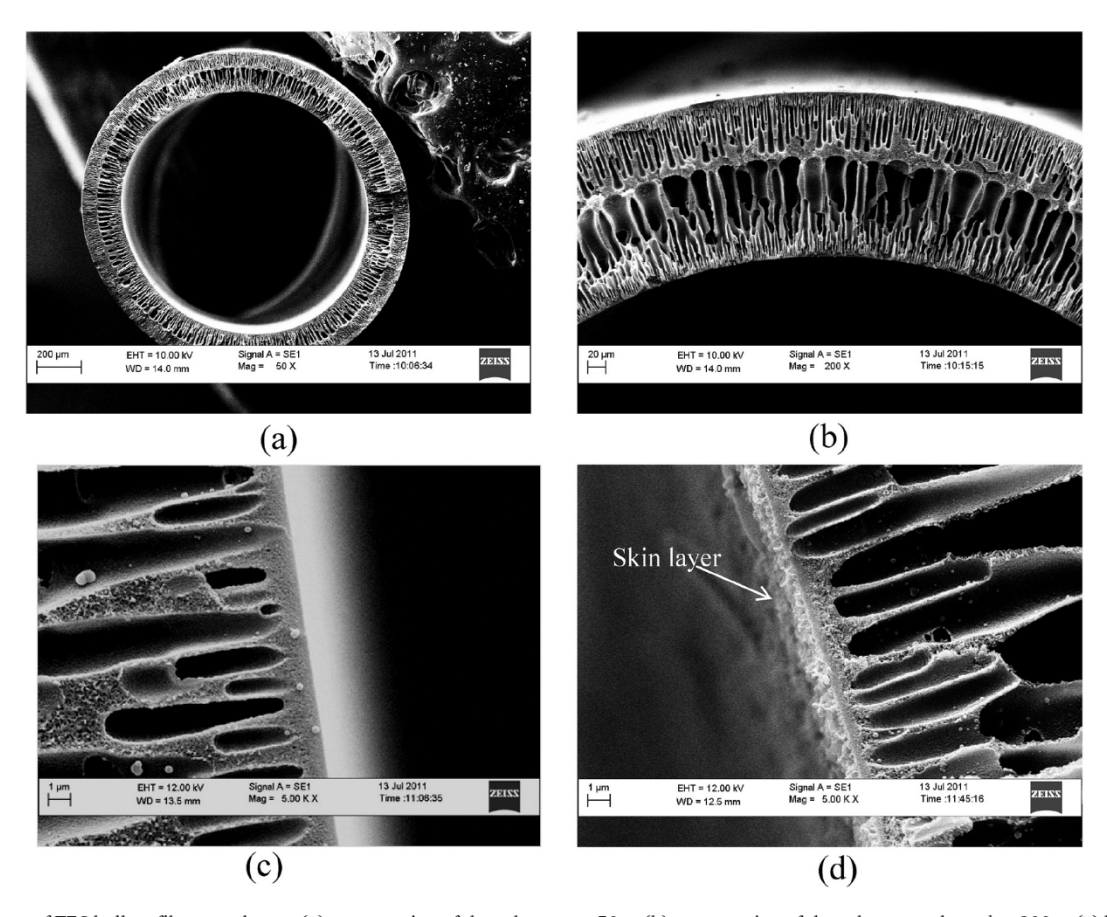


Fig. 6. Morphology of TFC hollow fiber membrane: (a) cross-section of the substrate at $50 \times$, (b) cross-section of the substrate enlarged at $200 \times$, (c) lumen side of the substrate enlarged at $5000 \times$, (d) lumen side of TFC hollow fibers enlarged at $5000 \times$. Different from figure c, figure d shows a uniform ridge-and-valley thin layer attached to the inner surface of the hollow fiber, which is a typical morphology of a polyamide thin-film hollow fiber synthesized by interfacial polymerization. Reprinted with permission from Ref. [58].

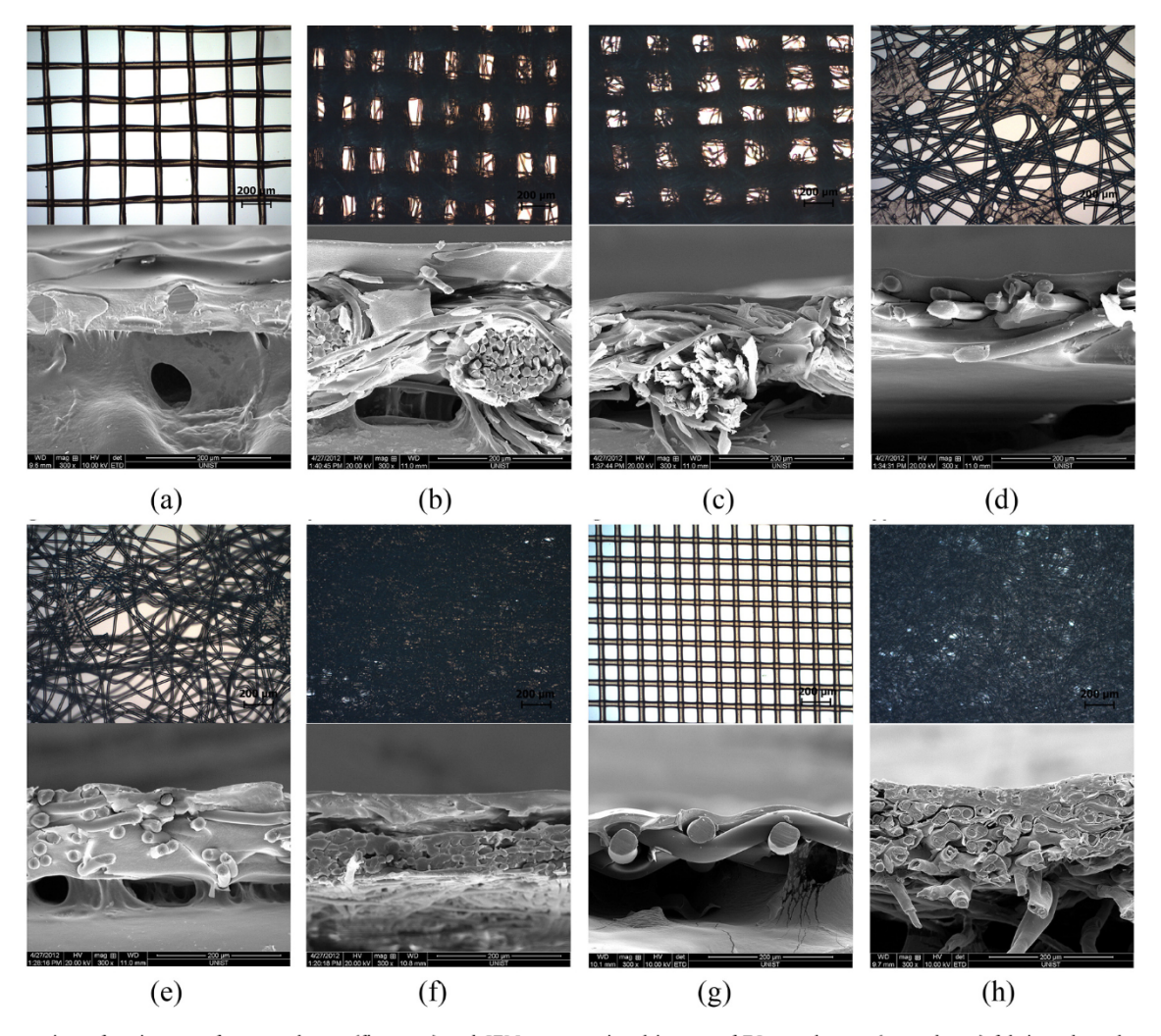


Fig. 7. Microscopic surface images of support layers (first row) and SEM cross-sectional images of FO membranes (second row) fabricated on the corresponding support layers. a, b, and c show different woven fabrics; d, e, and f show different nonwoven fabrics; g and h show two commercially available membranes obtained from Hydration Technology Innovations (HTI). Reprinted with permission from Ref. [86].

technology [56]. Therefore, these two power generation technologies are generally below the standard of commercialization, especially the FO-EK technology. Essentially, the lower-than-estimated power density is attributed to the lack of effective membranes with low CP, high salt rejection, high water permeation, and high mechanical strength [89]. Moreover, due to the difficulties in developing suitable and cost-efficient semipermeable membranes on a large scale, the investigations of the two power generation technologies have been limited to laboratories.

Great efforts have been paid to improve the performance of the currently available semipermeable membranes. Surface treatment on the semipermeable membranes to improve the properties of mass transfer and semipermeablility is always the main branch in osmosis studies [90,91]. For example, to mitigate the fouling of the TFC polyetherimide (PEI) hollow fiber membrane, Li et al. modified the outer surface of the inner-selective layer through depositing poly-(allylamine hydrochloride) (PAH) and poly acrylic acid (PAA) polyelectrolytes. The modified membrane had fewer exposed pores and was more negatively charged, which was beneficial for preventing the adsorption of the negatively charged foulants onto the membrane substrate [62]. Sun and Chung also reported synthesized outer-selective TFC hollow fiber membranes for the membrane-based indirect power generation process. After vacuum-assisted interfacial polymerization, the PRO performance is further enhanced by optimizing the support layer in terms of pore size and mechanical strength. The polydopamine-coated and mechanicallystrengthened membranes can stand over 2 MPa with a peak power

density of 7.63 $\rm W/m^2$ [92]. Further enhancement on the salt rejection and the robustness of the outer-selective TFC hollow fiber membranes boosted the peak power density up to 10.06 $\rm W/m^2$ [93]. Those studies provide insightful guidelines for optimizing the interfacial polymerization procedures and scaling up the TFC hollow fiber membrane modules for more PRO power generation.

3.1.2. The availability of DS

Although the energy at the estuary is enormous, the density of salinity gradient energy is relatively low and is around 0.256 kWh/m³ with the initial river water and seawater volume [94]. In addition, compared with the extraction of traditional energy sources, that of lowdensity energy requires more energy inputs and also leads to more energy losses. Particularly, the pumping energy to circulate the river water and the seawater and the energy required for pretreatment of the source fluids are estimated to be over 38% of the total energy inputs [95] and are the two main energy inputs during PRO power generation at the river mouth. In addition, the constant-pressure operation in a countercurrent module, the reverse salt flux, and the CPs, and the inefficiencies of the pressure exchanger and turbine lead to energy losses larger than 25%, 15%, and 9.5% of the extractable energy. As known, the energy input and the energy loss are the two main elements when calculating the energy conversion efficiency of the PRO system. Therefore, the expected net energy outputs achieved by the PRO power plant using the river water and the seawater are substantially lower. Straub et al. also draw a similar conclusion that the PRO cannot yield excellent energy conversion efficiencies no matter how many effective membranes and pretreatment methods are going to be explored [52]. This conclusion can rationally explain the reason why a Norwegian company Statkraft stopped all investments in pioneering the introduction of the PRO technology to the first full-scale plant [96]. In the FO-EK power generation process, the problem caused by the low extractable energy source at the river mouth is even more severe.

Although those two power generation technologies have been thoroughly analyzed and proved to be probably inefficient at the river-to-sea sites, they are proved promising at places with hypersaline sources. The hypersaline sources within the context of the research of osmosis power generation are commonly defined as solutions with concentrations ranging from 6 wt% (appr. 1 M NaCl solution) to 26 wt/wt% at 25 °C for experimentally prepared pure NaCl solution [97], 33-35 wt/wt% for natural salt mixtures (such as hypersaline lakes, salt domes, hypersaline geothermal water, etc.) [98], or 59 wt/wt% (appr. 7.6 M NaCl solution) for engineered solutions (such as desalination brine, wastewater brine, oil field brines, evaporation ponds, etc.) [99]. Utilizing the hypersaline sources as the DS can help to overcome the challenges mentioned above due to their unique properties of high energy densities and offer a potential route for commercialization [100,101]. Table 2 provides an overview of studies utilizing hypersaline solutions as the DS and fresh water, brackish water, or seawater as the FS for PRO power generation processes. It proves that the application of hypersaline sources can greatly enhance the power density. Furthermore, Helfer et al. gave a full overview of the potential hypersaline environments, such as Great Salt Lake in the USA, Lake Torrens in Australia, Lake Assal in Djibouti, Chott Melrhir in Algeria for PRO power production. The corresponding possible DS/FS pairs were also proposed as well as their approximate osmotic pressure difference and the estimated power output. Finally, the numbers of households supplied with generated electricity were also derived based on the average electricity consumption per capita in each country [102].

When the hypersaline sources are used as DS in membrane-based power generation processes, one important thing should be paid more attention to. Taking the PRO power generation process as an example, there is a peak power density in theory at an optimal applied pressure, which is generally accepted to be half of the effective osmotic pressure for the PRO power generation process as shown in Fig. 4. However, in experimental and industrial applications, if the concentration of NaCl DS is larger than 2 M, the corresponding optimal power density cannot be obtained due to the mechanical strength limitations of the semipermeable membranes. To be more specific, the further increment in the applied pressure leads to severe deformation or damage of the membrane. Furthermore, the increased applied pressure also blocks the permeation of the feed stream [36,103,104,111]. One effective strategy for further improvement of the PRO power generation performance with using hypersaline DS is to apply optimally designed FS spacers [103,118].

3.1.3. Operation mode

As known, the CP phenomenon is inevitable in the osmosis-driven membrane technologies and cannot be eliminated even in the most developed PRO or FO process. CP greatly reduces the solvent permeating flux and eventually decreases the generated power density, especially when it acts on both sides of the membrane. In addition, only part of the salinity gradient energy can be effectively recovered by the PRO or the FO process in real applications, and the remaining is discharged. However, the discharged effluent will lead to serious negative impacts on the environment if it is not post-processed properly [123]. Therefore, some innovative operation modes are needed to fully exploit the salinity energy and effectively reduce the CP phenomenon. Xu et al. investigated the PRO performance through a Hydrowell® spiral wound FO module (SWFO) under both submerged and crossflow conditions and found that the SWFO mode yields relatively good PRO performance under both

Table 2Overview of hypersaline solutions applied for PRO power generation processes.

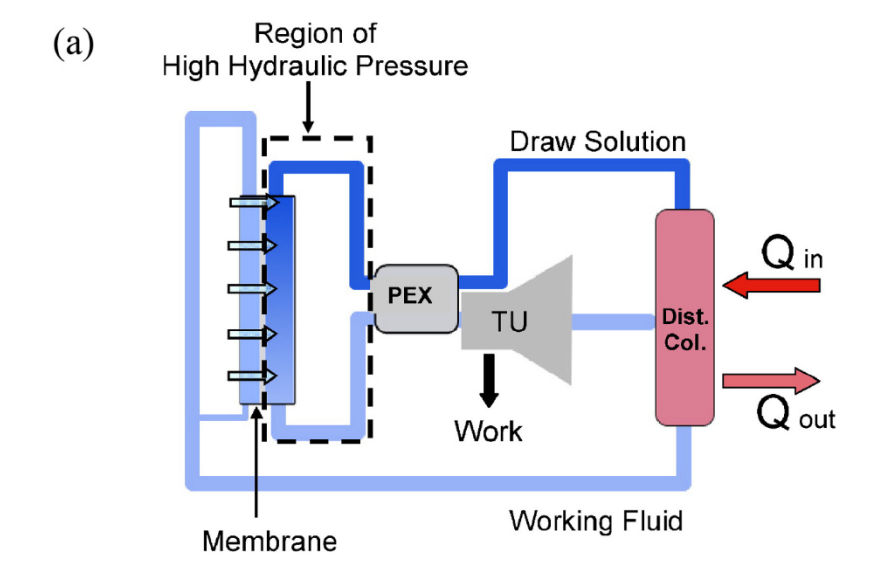
Seawater brine (1.06 M NaCl solution)	DS .	FS	Power density, W/m ²	Reference
2 M NaCl solution	M NaCl solution	10 mM NaCl	3.8	She and Tang ,
1 M NaCl solution				
2 M NaCl solution				
1 M NaCl solution				
1 M NaCl solution	, in read bolddon		3,00	,
Seawater brine (1.06 M NaCl solution)	. M NaCl solution	1 mM NaCl solution	20.9	Chou et al., 2013
Synthetic river water (0.9 mM NaCl solution)	•	water (80 mM NaCl	15.2	Song et al., 2013
NaCl solution O.5 M NaCl solution 4.7 Kim and Elimelech [107]		Synthetic river	21.3	
Elimelech [107] 1 M Na ₅ [Fe(C ₆ H ₄ O ₇) ₂]		NaCl solution)		
(Na-Fe-CA) hydroacid complex solution 1 M NaCl solution 10 mM NaCl solution 1 M NaCl solution DI water 24.3 2 Mang et al., 20 [110] 1 M NaCl solution DI water 24.3 2 M NaCl solution 39.4 [111] 3 M NaCl solution DI water 21.3 3 M NaCl solution 27 2015 [112] Seawater brine from the Tuaspring desalination plant 1.5 M NaCl solution DI water 11.2 2 Macl solution DI water 11.2 3 M NaCl solution DI water 11.2 4 M NaCl solution DI water 11.2 5 M NaCl solution DI water 11.2 5 M NaCl solution DI water 11.2 6 M NaCl solution DI water 11.2 7 M NaCl solution DI water 11.2 8 Anastasio et al 2015 [113] 1 M NaCl solution DI water 11.2 1 M NaCl solution DI water 11.2 2 Macl solution DI water 11.2 3 M NaCl solution DI water 12.8 5 Li, et al., 2015 [115] 0.81 M NaCl solution DI water 8.3 5 Kim et al., 201 [36] 0.81 M NaCl solution DI water 12.9 Wei et al., 201 [117] 3 M NaCl solution DI water 22.6 Hickenbottom				Elimelech [107]
Solution 10 mM NaCl 5.1 Fu et al., 2014 solution [109]	(Na-Fe-CA)	DI water	16.2	
1 M NaCl solution 10 mM NaCl solution 5.1 Fu et al., 2014 [109] 1 M NaCl solution DI water 24.3 Zhang et al., 20 [110] 1 M NaCl solution DI water 14.1 Straub et al., 20 [110] 2 M NaCl solution 39.4 [111] 3 M NaCl solution 59.7 0.81 M NaCl solution DI water 21.3 Wan and Chun 1 M NaCl solution 1 M NaCl solution 27 2015 [112] Seawater brine from the Tuaspring desalination plant 21.1 Anastasio et al. 2015 [113] 1 M NaCl solution DI water 18 Anastasio et al. 2015 [113] 1 M NaCl solution DI water 11.2 Chen et al., 201 [35] 1.2 NaCl solution DI water 8.06 Kim et al., 201 [35] 2 NaCl solution 10 mM NaCl 20.3 [114] 1 M NaCl solution DI water 8.3 Kim et al., 2015 [36] 0.81 M NaCl solution Wastewater from 7.7 Zhao et al., 20 [36] 0.81 M NaCl solution DI water 12.9 Wei et al., 201 [117] 3 M NaCl solution DI water 22.6 Hickenbottom				
1 M NaCl solution DI water 24.3 Zhang et al., 26 [110] 1 M NaCl solution DI water 14.1 Straub et al., 26 [110] 2 M NaCl solution 39.4 [111] 3 M NaCl solution 59.7 0.81 M NaCl solution 27.7 2015 [112] 1 M NaCl solution 27 2015 [112] 2015 [112] Seawater brine from the Tuaspring desalination plant 21.1 21.1 1.5 M NaCl solution DI water 18 Anastasio et al. 2015 [113] 1 M NaCl solution DI water 11.2 Chen et al., 20 [35] 1.2 NaCl solution DI water 8.06 Kim et al., 201 [36] 2 NaCl solution 10 mM NaCl 20.3 [114] Li, et al., 2015 [115] 2 M NaCl solution DI water 8.3 Kim et al., 201 [15] 2 M NaCl solution DI water 8.3 Kim et al., 20 [36] 0.81 M NaCl solution Wastewater from 7.7 Zhao et al., 20 [16] municipal recycle plants plants 1 M NaCl solution DI water 12.9 Wei et al., 201 [117] 3 M NaCl solution DI water 22.6 Hickenbottom	M NaCl solution		5.1	Fu et al., 2014
1 M NaCl solution DI water 14.1 Straub et al., 2 2 M NaCl solution 39.4 [111] 3 M NaCl solution 59.7 0.81 M NaCl solution 27 2015 [112] 1 M NaCl solution 27 2015 [112] Seawater brine from the Tuaspring desalination plant 21.1 21.1 1.5 M NaCl solution DI water 18 Anastasio et al. 2015 [113] 1 M NaCl solution DI water 11.2 Chen et al., 20 [35] 1.2 NaCl solution DI water 8.06 Kim et al., 201 [36] 2 NaCl solution 10 mM NaCl 20.3 [114] 1 Li, et al., 2015 [115] 2 M NaCl solution DI water 8.3 Kim et al., 201 [36] 2 M NaCl solution DI water 8.3 Kim et al., 201 [36] 0.81 M NaCl solution Wastewater from 7.7 Zhao et al., 20 [16] 1 M NaCl solution DI water 12.9 Wei et al., 201 [117] 3 M NaCl solution DI water 22.6 Hickenbottom	. M NaCl solution		24.3	Zhang et al., 2014
2 M NaCl solution 39.4 [111] 3 M NaCl solution 59.7 0.81 M NaCl solution 27 2015 [112] Seawater brine from the Tuaspring desalination plant 21.1 21.1 1.5 M NaCl solution DI water 18 Anastasio et al. 2015 [113] 1 M NaCl solution DI water 11.2 Chen et al., 20 2 NaCl solution DI water 8.06 Kim et al., 2015 2 NaCl solution 10 mM NaCl 12.8 Li, et al., 2015 1 M NaCl solution DI water 8.3 Kim et al., 2015 2 M NaCl solution DI water 8.3 Kim et al., 201 0.81 M NaCl solution Wastewater from municipal recycle plants 7.7 Zhao et al., 20 municipal recycle plants 1 M NaCl solution DI water 12.9 Wei et al., 201 3 M NaCl solution DI water 22.6 Hickenbottom	M NaCl solution	DI water	141	
3 M NaCl solution 59.7 0.81 M NaCl solution DI water 21.3 Wan and Chun 1 M NaCl solution 27 2015 [112] Seawater brine from the Tuaspring desalination plant 21.1 21.1 1.5 M NaCl solution DI water 18 Anastasio et al. 2015 [113] 1 M NaCl solution DI water 11.2 Chen et al., 20 2 NaCl solution DI water 8.06 Kim et al., 201 2 NaCl solution 10 mM NaCl 12.8 Li, et al., 2015 3 M NaCl solution DI water 8.3 Kim et al., 201 4 M NaCl solution DI water 8.3 Kim et al., 201 5 M NaCl solution Wastewater from municipal recycle plants 7.7 Zhao et al., 201 1 M NaCl solution DI water 12.9 Wei et al., 201 1 M NaCl solution DI water 22.6 Hickenbottom		DI Water		,
0.81 M NaCl solution DI water 21.3 Wan and Chun 1 M NaCl solution 27 2015 [112] Seawater brine from the Tuaspring desalination plant 21.1 21.1 21.1 21.1 21.1 21.1 21.1 21.1 21.2 21.2 21.2 21.2 21.2 20.2 20.2 20.2 20.2 20.2 20.2 20.2 20.2 [35] 2.2 3.2 2.2 3.2 2.2 3.2 2.2 3.2				[111]
1 M NaCl solution 27 2015 [112] Seawater brine from the Tuaspring desalination plant 21.1 1.5 M NaCl solution DI water 18 Anastasio et al. 2015 [113] 1 M NaCl solution DI water 11.2 Chen et al., 20 [35] 1.2 NaCl solution DI water 8.06 Kim et al., 201 [35] 2 NaCl solution 10 mM NaCl 20.3 [114] 1 M NaCl solution 10 mM NaCl 20.3 [115] 2 M NaCl solution DI water 8.3 Kim et al., 2015 [36] 0.81 M NaCl solution Wastewater from municipal recycle plants 7.7 Zhao et al., 20 municipal recycle plants 1 M NaCl solution DI water 12.9 Wei et al., 201 [117] 3 M NaCl solution DI water 22.6 Hickenbottom		DI		W
Seawater brine from the Tuaspring desalination plant 1.5 M NaCl solution DI water 18		DI water		-
Tuaspring desalination plant 1.5 M NaCl solution DI water 18 Anastasio et al. 2015 [113] 1 M NaCl solution DI water 11.2 Chen et al., 20 [35] 1.2 NaCl solution DI water 8.06 Kim et al., 201 [35] 2 NaCl solution 20.3 [114] 1 M NaCl solution 10 mM NaCl 12.8 Li, et al., 2015 [36] 2 M NaCl solution DI water 8.3 Kim et al., 201 [36] 0.81 M NaCl solution Wastewater from municipal recycle plants 7.7 Zhao et al., 20 [116] 1 M NaCl solution DI water 12.9 Wei et al., 201 [117] 3 M NaCl solution DI water 22.6 Hickenbottom				2015 [112]
1.5 M NaCl solution	Tuaspring		21.1	
1 M NaCl solution DI water 11.2 Chen et al., 20 [35] 1.2 NaCl solution DI water 8.06 Kim et al., 201 [114] 2 NaCl solution 10 mM NaCl 12.8 Li, et al., 2015 [115] 2 M NaCl solution DI water 8.3 Kim et al., 201 [36] 0.81 M NaCl solution Wastewater from municipal recycle plants 7.7 Zhao et al., 20 [116] 1 M NaCl solution DI water 12.9 Wei et al., 201 [117] 3 M NaCl solution DI water 22.6 Hickenbottom	-	DI water	18	Anastasio et al.,
1.2 NaCl solution DI water 8.06 Kim et al., 201 2 NaCl solution 20.3 [114] 1 M NaCl solution 10 mM NaCl 12.8 Li, et al., 2015 solution [115] 2 M NaCl solution DI water 8.3 Kim et al., 201 [36] 0.81 M NaCl solution Wastewater from municipal recycle plants 7.7 Zhao et al., 20 1 M NaCl solution DI water 12.9 Wei et al., 201 [117] 3 M NaCl solution DI water 22.6 Hickenbottom	M NaCl solution	DI water	11.2	Chen et al., 2015
2 NaCl solution 20.3 [114] 1 M NaCl solution 10 mM NaCl 12.8 Li, et al., 2015 solution [115] 2 M NaCl solution DI water 8.3 Kim et al., 201 [36] 0.81 M NaCl solution Wastewater from municipal recycle plants [116] 1 M NaCl solution DI water 12.9 Wei et al., 201 [117] 3 M NaCl solution DI water 22.6 Hickenbottom	.2 NaCl solution	DI water	8.06	
1 M NaCl solution 10 mM NaCl solution 12.8 Li, et al., 2015 2 M NaCl solution DI water 8.3 Kim et al., 2016 36] 0.81 M NaCl solution Wastewater from municipal recycle plants 7.7 Zhao et al., 20 1 M NaCl solution DI water 12.9 Wei et al., 2016 1 M NaCl solution DI water 22.6 Hickenbottom				
Solution [115]		10 mM NaCl		
2 M NaCl solution DI water 8.3 Kim et al., 201 [36] 0.81 M NaCl solution Wastewater from municipal recycle plants 7.7 Zhao et al., 20 [116] 1 M NaCl solution DI water 12.9 Wei et al., 201 [117] 3 M NaCl solution DI water 22.6 Hickenbottom	. III IIII SOIGIOII		12.0	
0.81 M NaCl solution Wastewater from 7.7 Zhao et al., 20 municipal recycle [116] plants 1 M NaCl solution DI water 12.9 Wei et al., 201 [117] 3 M NaCl solution DI water 22.6 Hickenbottom	M NaCl solution		8.3	Kim et al., 2015
1 M NaCl solution DI water 12.9 Wei et al., 201 [117] 3 M NaCl solution DI water 22.6 Hickenbottom	0.81 M NaCl solution	municipal recycle	7.7	Zhao et al., 2016
3 M NaCl solution DI water 22.6 Hickenbottom	M NaCl solution	•	12.9	Wei et al., 2016
	3 M NaCl solution	DI water	22.6	
			18.73	Bader et al., 2016
	Brine from desalination		13.5	Kurihara et al.,
Concentrated brine 17.1 (ca.7%)	Concentrated brine		17.1	_010 [120]
	` '	DI water	20	Wan et al., 2017
	Brine from seawater	Red Sea water	1.97	Khasawneh et al.,
desalination plants Treated water 2.2 2018 [122]				
Dead Sea water Red Sea water 58.7				()

conditions with feed water being circulated outside the membrane envelope [124]. Jiao et al. also tried to weaken the negative effect of CP by utilizing a pump in the FO submodule to refresh the DS and thus enhance the osmosis process [15]. To make the PRO power generation system more productive, a PRO power generation system with a dual-stage operation mode was developed with different membrane module arrangements in the first and the second stages of the PRO processes [125–128]. It was demonstrated that this operation mode could sharply increase the chemical potential difference and reduce the CP on the FS side and thus yields higher specific electric energy, up to 16% of

increment for Dead Sea-RO brine [126].

Other major shortcomings of the PRO utilizing traditionally investigated river water and seawater are the costive pretreatments [129] and the relatively low effectiveness of osmotic pressure differences [61]. These negative aspects of the traditional PRO process stimulate investigations on novel conceptual operation modes such as the closed-loop PRO. McGinnis et al. developed an osmotic heat engine (OHE) to generate electricity, which is essentially a closed-loop PRO process, as shown in Fig. 8.a. This engine uses a concentrated ammonia-carbon

dioxide solution and DI water as DS and FS, respectively, to create high osmotic pressures, which induce water flux through a semipermeable membrane. The depressurization of the DS in a turbine produces electrical power. Meanwhile, heat is introduced to the diluted DS stream to separate the solutes from the DS, resulting in renewed DS and FS streams [130]. Han and Chung also developed a novel closed-loop PRO process to continuously convert the osmotic energy into electricity with recovering the diluted DS through the precipitation process. As shown in Fig. 8.b, a $Na_5[Fe(C_6H_4O_7)_2]$ (Na-Fe-CA) hydroacid complex solution



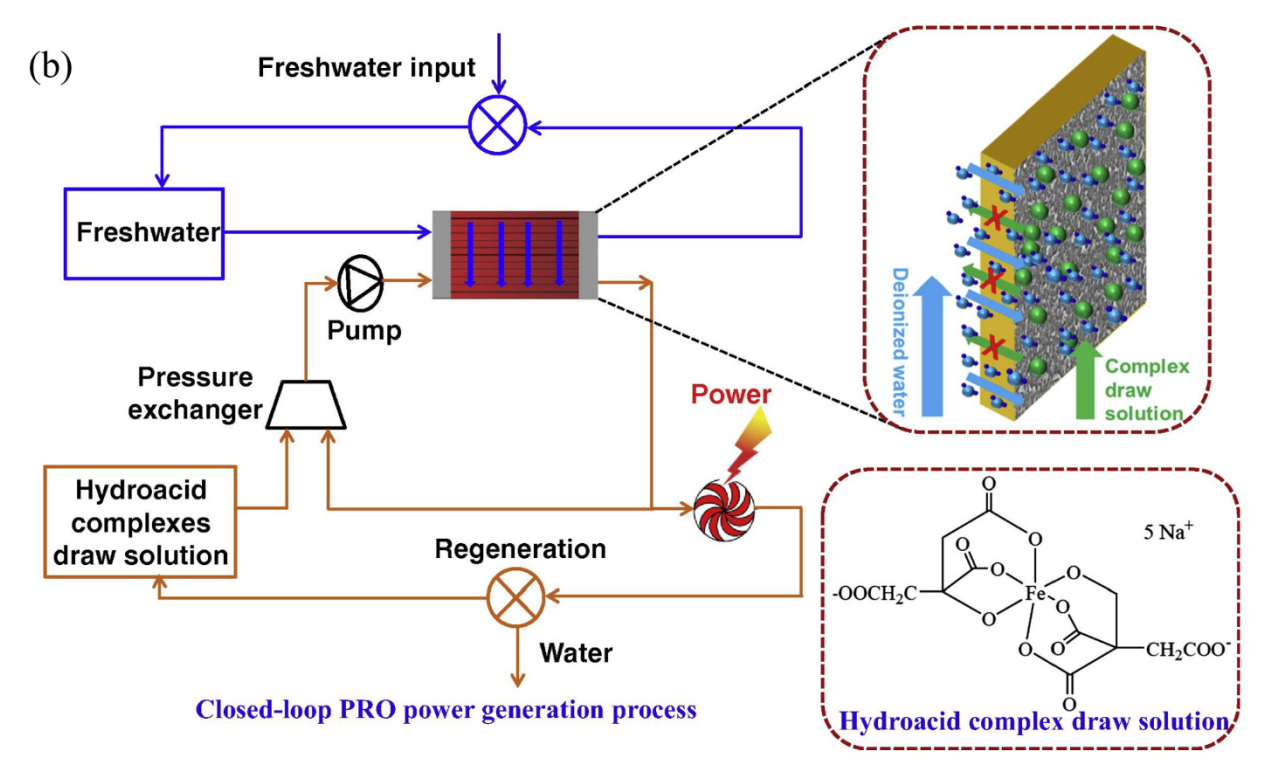


Fig. 8. Schematic of typical closed-loop PRO power generation processes. (a) The ammonia-carbon dioxide osmotic heat engine (OHE) for PRO power generation. A highly concentrated NH_3/CO_2 and a DI water are utilized as DS and FS to induce a high osmotic pressure difference. PEX and TU represent pressure exchanger and turbine, respectively. Q_{in} and Q_{out} denote the heat that flows into and out of the engine. Reprinted with permission from Ref. [130]. (b) The closed-loop PRO process for power generation and the Na-Fe-CA hydroacid complex as DS. The diluted hydroacid complex is recovered through the precipitation process. Reprinted with permission from Ref. [108].

with high water flux and negligible reverse solute flux was synthesized as DS. The water in the diluted complex DS can be extracted by ethanol, and the solute will be precipitated out of the water. The remaining water/ethanol in the mixture can be further removed by evaporation, and then the solute can be fully regenerated [108]. Compared to conventional PRO processes, the newly developed closed-loop PRO processes exhibit promising advantages of sustainable high power output, low membrane fouling, and, most importantly, remarkably low cost in pretreatment and brackish water discharge.

3.1.4. Solution temperature

Practically, the temperature of the FS/DS passing through the osmosis system may vary over a wide range, depending on the solution sources and the locations [131–133]. This parameter also plays an important role in those two power generation processes since it not only affects physicochemical properties of the solution, such as osmotic pressure, viscosity, density, and diffusivity but also affects the permeating performance of the membrane [134,135]. Therefore, it is meaningful to systematically investigate the effects of solution temperature on the performance of the PRO power generation processes.

Currently, only few studies investigated the effects of temperature on the mass transportation performance of the osmosis processes. Kim and Elimelech investigated the effect of solution temperature on the water flux and power density in PRO and found that increasing the solution temperature from 20 $^{\circ}\text{C}$ to 30 $^{\circ}\text{C}$ improved the water flux from 9.23 to $13.89 \text{ L/m}^2/\text{h}$ and elevated the power density from 3.22 to 4.72 W/m² for solution pair of 2 M NaCl DS/0.5 M NaCl FS [107]. Touati et al. also studied the effects of the bulk solution temperature on the PRO power generation processes and found that, compared with the DS temperature, the FS temperature has more significant influences on the membrane performance during the PRO processes [136]. This conclusion coincides with that reported by Abdelkader and Sharqawy [137]. In addition, the power density was found to be increased by about 130% when both feed solution and draw solution temperatures increase from 20 °C to 50 °C [137]. Overall, although the increase of the water permeating flux is accompanied by a high salt diffusion which leads to a severe ICP [136], the expected power density is improved with the increment of the FS temperature [138].

3.2. The electric submodule

3.2.1. In PRO power generation system

In the PRO power generation system, an electric submodule is required to generate electricity, which includes turbine, generator, pressure exchanger, and their mechanical components, as shown in Fig. 3. Turbine and generator have already been fully developed, and their efficiencies can be achieved over 90% [139]. The operation of the turbine and generator in the PRO power generation system is similar to that in the ordinary hydraulic power generation system. The pressurized DS from the osmosis submodule runs through the turbine, and then the connected generator generates electric power. It is reported that further performance improvement of the turbine and the generator can be achieved by around 3%. In the PRO power generation process, the solution exhausted from the turbine is called the mixed brine or brackish water, which might contain undesirable chemicals after passing through the system. Therefore, post-treatment for the brackish water is necessary before being discharged to the source. In addition to these two main components in the electric submodule, the pressure exchangers are also necessary and are utilized to transfer the pressure from the mixed DS to the inflow of the original DS so that the power consumption of the system can be reduced and the overall energy conversion efficiency can be potentially increased in the long run [140]. Consequently, the improvement in operational efficiencies of the components and the recovery of the energy from the exhausted streams in the electric submodule will boost the performance of the whole power generation system.

One interesting thing is that almost all studies on the PRO power generation technologies only detailedly investigate the performance of the membrane submodule and then achieve the corresponding energy conversion performance based on theoretical derivation on the electric submodule. Therefore, the study on the complex performance of the complete PRO system combining the membrane submodule and the electric submodule should be conducted in the future for its large-scale applications.

3.2.2. In FO-EK power generation system

Similar to the PRO power generation systems, FO-EK power generation systems also require an electric submodule to generate electricity. The functional element of the electric submodule works based on the interfacial electro-chemical mechanism of the pressure-driven EK flow with main electric features of the streaming potential and the streaming current. Both the streaming potential and the streaming current have been intensively studied for developing microfluidic devices such as flow rate meters, pressure sensors, particle manipulation techniques, etc. [141] and have started to be innovatively exploited in the field of EK batteries in recent years. The energy conversion performance and the weaknesses and challenges of this novel micro/nano-power generator should be investigated thoroughly.

3.2.2.1. The size of the nanochannel. According to current experimental studies, the maximum energy conversion efficiency of the FO-EK technology is only around 3.08 W/m3 by using the porous glass with an average pore size of $6 \mu m$ [78]. It is known that the energy conversion efficiency of the pressure-driven EK flow strongly depends on the radius of the channel. Particularly, the energy conversion efficiency reaches the maximum when the radius of the channel is around two times the EDL thickness and decreases sharply when the radius of the channel deviates from the critical radius [72]. The EDL thickness is from 3.04 nm to 304 nm for the symmetric electrolyte solution such as NaCl or KCl solution with a concentration from 10 mM to 10^{-3} mM . Therefore, the channel size, in general, should be at least below 1 μm so that a maximum energy conversion efficiency can be promisingly achieved. Accordingly, the energy conversion performance of the FO-EK technology can be improved by exploring proper porous media or EK membrane with suitable pore size to provide efficient nanochannels. With the developments in MEMS packaging technologies, lots of novel artificial nanochannel devices are developed, such as the glass microchannel array [142,143], polyelectrolytic AAO membranes [144-146], mixedcellulose membrane filter [147,148], etc. to directly or indirectly test the properties such as streaming potential and/or streaming current. Further attempts to enhance the energy conversion efficiency of the FO-EK system can be taken by replacing the currently applied porous glass with the one with smaller pore size, the nanochannel devices mentioned above, or other related advanced membranes.

3.2.2.2. The slip boundary condition. It was recently proposed that the slip boundary condition on hydrophobic surfaces could significantly enhance the electroosmosis performance in nanochannels [77], and this hypothesis was experimentally verified [74,75]. It is known that there are mainly two kinds of friction in microfluidics, namely, the friction resulting from the interaction between the solvent and the wall and the friction resulting from the interaction between the solute and the wall. Water molecules with low density occurring in the vicinity of hydrophobic surfaces decrease the interaction between the water molecules and the wall [149]. Hence, water can flow over the hydrophobic wall more smoothly, giving rise to a non-zero boundary velocity. Compared with the common wetting case with non-slip boundary conditions, the non-wetting case with slip boundary conditions was more intensively investigated both theoretically and experimentally [77,150-153]. It was found that the charges within the Stern layer, usually immobile in the case of a hydrophilic wetting surface, can flow over hydrophobic

surfaces due to the slip condition. As a result, the streaming current is greatly enhanced in addition to the increment of the mean velocity within the channel due to the slip velocity at the interface. Under the condition of constant surface charge density, the relatively high hydrophobicity of the solid surface can enhance the EK phenomena by a slip-induced amplification factor of $(1+b/\lambda_{eff})$, where λ_{eff} and b are the effective Debye length and the slip length, respectively [74,76]. Although such a kind of boundary condition may not be as precise as that in previous modelings with constant surface charge [69,73], the expression of the slip-induced amplification factor shows a more qualitative understanding of the effects of liquid slip on the pressure-driven EK flow in microfluidics.

A highly hydrophobic solid surface gives rise to high liquid velocity and thus low pressure consumption. In addition, high surface charge density induces a high zeta potential. Ideally, improvements in both of these two aspects can greatly enhance the EK flow in micro/nanochannels. However, it is known that the less polarizable the solid surface molecules are, the more hydrophobic the solid surface is. In other words, the solid surface hydrophobicity can be increased by diminishing surface charge density [154,155], which, however, simultaneously reduces the zeta potential. There is a common tradeoff between strong slip and high surface charge density. To improve the energy conversion performance of the pressure-driven EK flow, we try to enhance the slip condition of the micro/nano-channels while increasing or maintaining at least the surface charge density. How to practically balance these two aspects to achieve better hydrodynamic and EK performance of the microfluidic system is the most challenging issue for current and future research in this field.

Two reported promising surface treatment methods are recommended for future study. The first one is the treatment of silica micro/nano-channel with carboxyl groups. It has been proved that compared to the original silica material with a zeta potential of $-42 \, \mathrm{mV}$, the silica material modified by carboxyl groups exhibits an increased zeta potential up to $-72 \, \mathrm{mV}$ almost without alteration of the wetting property [156]. The second one is the treatment of silica micro/nano-channel with poly (propylene glycol) methacrylate. The zeta potential of the modified silica material is almost not affected while the ability to adsorb water molecules significantly decreases, greatly enhancing the hydrophobicity [157].

3.2.2.3. The two-phase flow. According to the traditional theory of the streaming current in single-phase systems, the internal conduction current induced by the streaming potential limits the output power, which ultimately diminishes the energy conversion efficiency of the pressure-driven EK flow. The use of a certain two-phase flow, as shown in Fig. 9, can effectively overcome this problem. Xie et al. studied the energy conversion performance of a pressure-driven EK flow using a two-phase flow, the N_2 -KCl solution (1 mM) bubble flow. A gas source (99% purity N_2) was used to drive the liquid flow and to generate gas bubbles. Their study shows that in a two-phase system, the bubbles

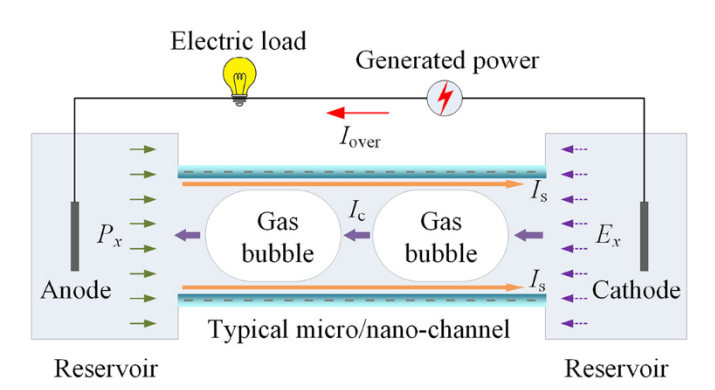


Fig. 9. Schematic of the bubble flow through a micro/nano-channel.

greatly reduce the conduction current, increasing the output power. The addition of bubbles enhances the maximum output power by a factor of 74 and the energy conversion by a factor of 163 than that in a single-phase flow [158].

3.2.2.4. The non-Newtonian nanofluids. Non-Newtonian nanofluids, such as polymer solutions and colloidal suspensions, contain discrete entities on the nanoscale, which can be used as flow media for the electroosmosis flow. Compared to simple electrolyte solutions, they can give rise to higher thermodynamic efficiency [159]. As shown in Fig. 10, when such kind of non-Newtonian nanofluids is forced to pass through a micro/nano-channel by a pressure gradient, a certain degree of wall depletion will happen at the interfacial region. It forms a depletion layer. If the thickness of EDL is smaller than that of the depletion layer, the streaming current will be free of the macromolecules or nanoparticles in the bulk liquid. It is known that the viscosity of non-Newtonian nanofluids is a function of the shear rate and has been proved to be always higher than the viscosity of simple electrolyte solution [160]. In other words, if proper polymer solutions are utilized in such a micro/nanochannel, the viscosity of the nanofluids in the bulk region must be relatively higher than that in the depletion layer. In addition, the maximum energy conversion efficiency for the case of $\lambda \ll a$ can be approximated as $E_{\text{FO-EK,max}} = \alpha_{12}^2/(4\alpha_{11}\alpha_{22})$ [68,161–163]. It is observed from the expressions of all coefficients that the method of adding water-soluble polymer or nano-particles into the background electrolyte solution can reduce the coefficient α_{22} without altering α_{12} . The energy conversion efficiency is thus increased. Nguyen et al. firstly investigated the effects of the polymer solutions on the energy conversion efficiency of the pressure-driven EK process with experiments [164]. Their experiments show that, with adding polyacrylic acid (PAA) into a 0.01 mM KCl solution with a concentration of 200 ppm to 4000 ppm, the energy conversion efficiency of the system was extremely enhanced by a factor of 447 ($\pm 2\%$) than that in the case with only 0.01 mM KCl solution. Therefore, it is recommended to explore and investigate more suitable non-Newtonian nanofluids to increase the energy conversion efficiency of the pressure-driven EK process in future studies.

3.2.2.5. The surface texture of the channel. In addition to the porous glass, membranes with densely compacted micro/nano-channel arrays, as shown in Fig. 11, can also be used as the media to provide micro/nano-channels for superior performance of the pressure-driven EK flow. It is reported that the EK energy conversion of flow work to electricity using a glass microchannel array could achieve a maximum power output of 1 mW with an efficiency of 1.3% [142]. Meanwhile, recent studies report that the textured channel surfaces comprised of grooves filled with air or liquid can significantly increase the streaming potential by as high as 150% due to transverse pressure gradients [165,166]. It is argued that such tunability of the streaming potential

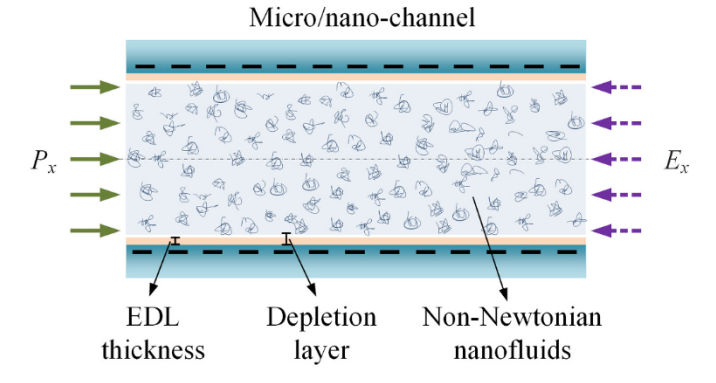


Fig. 10. Schematic of the EK flow of a non-Newtonian nanofluid through a micro/nano-channel.

Typical micro/nano-channel

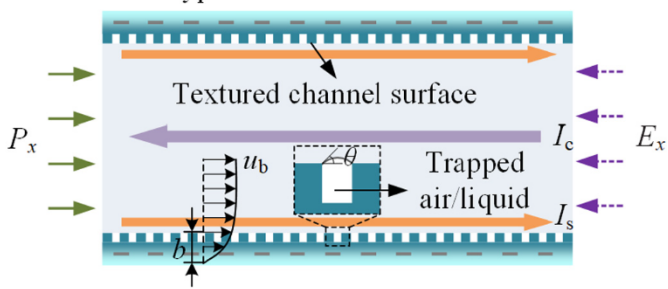


Fig. 11. The schematic of the pressure-driven EK flow through a micro/nano-channel with a textured channel surface. u_b , θ , and b are the bulk velocity of the flow, the protrusion angle, and the apparent slip length, respectively.

may be related to a variation in the local apparent slip characteristics and the surface charge density of the air-filled surfaces or the liquid-filled surfaces. In fact, one earlier numerical study using lattice Boltzmann simulations already proves that the apparent slip properties of the channel can be tailored by changing the protrusion angle θ and the surficial structure pattern confined between two parallel walls. The maximum slip length larger than 100 nm for rhombic, rectangular, and square patterns is achieved when the protrusion angle equals zero [167]. Therefore, future improvements of energy conversion efficiency can focus on developing effective EK membranes with densely compacted micro/nano-channel arrays with different textured channel surfaces.

Besides, it is known that the high slippage and high surface charge density are crucial for good energy conversion performance from salinity gradient energy. However, they are hardly achieved at the same time. Recently, with the systematical review of the concept "Soft interface" in the field of the EK energy conversion, simultaneity enhancement in both aspects becomes possible [168]. The structure of the "Soft interface" channels happened to coincide with the structure shown in Fig. 11. Compared with the traditional micro/nano-channel surface, a soft interface within the micro/nano-channel endows micro/nanochannel with more desirable features by some specially designed surface modifications or the introduction of chemical additions or surfactants. The soft interface with altered solid-liquid or the liquid-liquid interactions within the micro/nano-channels greatly improves the surface charge densities and/or slippage and thus potentially enhances the energy conversion processes. Importantly, that study mentioned above also thoroughly summarized the methodologies in achieving such soft interface conditions within the micro/nano-channels, which facilitates further development of the salinity gradient energy conversion from the point of view of the nanofluidic devices.

4. Potential applications

As aforementioned, the membrane-based indirect power generation processes may not be viable at the estuary but can be applied at locations where hypersaline sources occur [107,169–174]. In this situation, electricity can be generated from the mixing of the hypersaline sources with the rivers or the oceans while effluent treatment and environmental protection are achieved simultaneously. Therefore, depending on different DS/FS sources, different operation schemes and protocols of the membrane-based indirect power generation technologies should be elaborately designed.

The natural hypersaline sources are promising candidates to be applied as DS in the osmosis process. Tran et al. provided a comprehensive investigation of the feasibility of key technical and financial parameters of a virtual 25 MW PRO power plant in a hypersaline environment, the Great Salt Lake in Utah, USA [175]. The high salinity of the lake (24% salt concentration on average) is a critical factor making the osmotic power plant economically feasible. The net annual energy

production is estimated to be 154,249 MWh. The capital cost is \$238.0 million, and the operation and maintenance cost is \$35.5 million per year. The levelized cost of electricity (LCOE) would be 0.2025/kWh, and further design improvements would reduce the LCOE to 0.1034/kWh

In addition, the combination of the membrane-based indirect power generation processes with other industrial processes also provides mutual benefit for sustainable power production and advanced wastewater treatment [176-180]. Bemporad proposed a hybrid scheme that coupled a PRO process into a solar pond (SP) energy conversion process in 1992 and found that the coupled scheme can significantly recover parts of the energy lost from unavoidable evaporation during the SP process [181]. The desalination of the seawater by reverse osmosis (SWRO) can generate a large amount of hypersaline brine [182,183]. However, additional energy is required to post-process this kind of environmentally hazardous effluent to meet the wastewater-discharging standard [184,185]. As a kind of artificial hypersaline source, desalination brine has already shown promising potential for pilot-scale application in the field of SWRO-PRO co-generation systems [23,24,186–190]. Researchers reasonably utilized hypersaline brine by coupling the SWRO system with a PRO power generation system, which not only recycles the effluent but also primarily dilutes the hypersaline brine to relatively normal wastewater. Altaee et al. also investigated the performance of the co-generation SWRO-PRO process for power generation and seawater desalination and found that up to 31% of the power consumed during the desalination process can be successfully made up for by the SWRO-PRO system [191]. Recently some studies have shown that the hybrid SWRO-PRO configuration can further bring down the net specific energy consumption by up to 50% in comparison with standard SWRO desalination systems [192,193].

The FO-EK energy conversion technology can also be potentially applied to power systems with larger scales, such as desalination plants, cars, and household appliances, due to its unique power generation mechanism. Meanwhile, this technology is more applicable in the field of portable power generators for mobile electronics [194], self-powered micro/nano-machines, wearable devices, etc. However, this technology is at the initial stage of development, and the corresponding FO-EK system is still facing lots of challenges before it can be commercially realized. Firstly, cost-effective and efficient membrane materials designed for large-scale FO and EK processes are required. Secondly, robust designs for the FO-EK system should be explored to withstand the harsh solution resource under real working conditions. Finally, the packaging scheme of the FO-EK setup should be further developed for simple and compact structure, low cost, high safety, high separation efficiency, and convenient installation, replacement, and maintenance of the pipes.

In brief, the membrane-based indirect energy conversion processes have great potential to be applied at the hypersaline regions or to be coupled with industrial processes. It can reasonably harvest salinity energy and thus effectively reduce desalination costs, mitigate the environmental impact, and, importantly, compensate for the energy consumption of some industrial processes.

5. Conclusion

This paper firstly conducts a comprehensive review of green membrane-based indirect power generation technologies, namely the traditional PRO and the newly emerging FO-EK, for harvesting salinity gradient energy from the viewpoint of membrane science. Firstly, a comprehensive introduction to the fundamentals of osmosis is given. Then, the working principles, the development, and the energy conversion performance of these two typical technologies are elaborated. Furthermore, the challenges and the corresponding promising solutions are reviewed in detail. The essential findings are outlined as follows.

- (i) Efficient semipermeable membranes with minimum concentration polarization, maximum salt rejection, maximum water permeation, and maximum mechanical strength are urgently required to boost the industrialization of the membrane-based indirect power generation technologies;
- (ii) The commonly discussed applications of the membrane-based indirect power generation technologies at the estuary where river water mixing with seawater is proved to be infeasible. Available hypersaline sources and the corresponding technical protocols should be explored for the pilot-scale application of the membrane-based indirect power generation processes;
- (iii) The operation modes in the osmosis submodule, such as the spiral wound mode and the dual-stage mode, are demonstrated to be helpful in sharply increasing the chemical potential difference and reducing the CP on the FS side, and thus yield higher specific electric energy;
- (iv) The expected power density is expected to be potentially improved by increasing solution temperatures;
- (v) The complex performance of the complete PRO system combining the membrane submodule and the electric submodule should be systematically analyzed in the future for further commercialization purposes;
- (vi) Available strategies to further improve the performance of FO-EK system include but are not limited to reducing the size of the nanochannel, enhancing the slippage and the surface charge of the nanochannel, utilizing two-phase flow and/or non-Newtonian nanofluids, etc.;
- (vii) The integration of the membrane-based indirect power generation technologies with the other main industrial processes provides mutual benefit for sustainable power production and advanced wastewater treatment.

Those interesting findings above inspire a promising perspective on the future development directions in both the fundamentals and the applications. As for the fundamentals, the theoretical model for the osmosis submodule should be further developed to cover the situation of hypersaline sources. Meanwhile, the theoretical model for the electric submodule, particularly for the case of the EK energy conversion process, should be further explored to be applicable for complex working conditions such as the two-phase flow and the non-Newtonian nanofluids. Furthermore, the complete theoretical model for the membranebased indirect energy conversion system should be improved and refined to cover both the osmosis and the electric generation processes. Importantly, the effects of solution temperature should also be considered in the overall theoretical model. As for future applications, the membrane-based indirect energy conversion processes have great potential to be applied at the hypersaline regions. From the viewpoint of the scale, the membrane-based indirect energy conversion technology shows unique advantages when being integrated with both the largescale scenarios, such as desalination plants and chemical plants, and the mobile scenarios such as cars and portable electronics.

In general, the membrane-based indirect energy conversion technologies should be regarded as an efficient supplementary way for green energy harvesting. However, there is still a long way to understand, explore, optimize, and simplify such energy conversion processes and the corresponding systems. Essentially, the largest challenge in current research on the membrane-based indirect power generation technologies lies in the scaling-up process from the lab-scale demonstration research to the large-scale commercialization under the limitation of inefficient membranes.

Declaration of competing interest

The authors declare that they have no known competing financial interests or personal relationships that could have appeared to influence the work reported in this paper.

Acknowledgments

This work was supported by the National Natural Science Foundation of China [grant numbers 52106246, 52106046, 51976157]; the National Defense Pre-Research Foundation of China [grant number 50910020100]; and the Natural Science Foundation of Jiangsu Province [grant numbers BK20200687, BK20200680].

References

- D.J. Rankin, D.M. Huang, The effect of hydrodynamic slip on membrane-based salinity-gradient-driven energy harvesting, Langmuir 32 (2016) 3420–3432, https://doi.org/10.1021/acs.langmuir.6b00433.
- [2] L.H. Yeh, F. Chen, Y.T. Chiou, Y.S. Su, Anomalous pH-dependent nanofluidic salinity gradient power, Small 13 (2017) 1702691, https://doi.org/10.1002/ smll.201702691, n/a.
- [3] G.Z. Ramon, B.J. Feinberg, E.M.V. Hoek, Membrane-based production of salinity-gradient power, <sb:contribution><sb:title>Energy Environ. </sb:title></sb:contribution><sb:host><sb:sseries><sb:title>Sci.</sb:title></sb:series></sb:sseries></sb:sseries></sb:title>Interpretable (2011) 4423–4434, https://doi.org/10.1039/clee01913a.
- [4] S. Loeb, Production of energy from concentrated brines by pressure-retarded osmosis: I. Preliminary technical and economic correlations, J. Membr. Sci. 1 (1976) 49–63, https://doi.org/10.1016/S0376-7388(00)82257-7.
- [5] P. Pourmovahed, J. Maisonneuve, Thermodynamic limits of using fertilizer osmosis to produce mechanical work via pressure retarded osmosis, J. Membr. Sci. 629 (2021), 119268, https://doi.org/10.1016/j.memsci.2021.119268.
- [6] M. Tawalbeh, A. Al-Othman, N. Abdelwahab, A.H. Alami, A.G. Olabi, Recent developments in pressure retarded osmosis for desalination and power generation, Renew. Sustain. Energy Rev. 138 (2021), 110492, https://doi.org/ 10.1016/j.rser.2020.110492.
- [7] R.E. Pattle, Production of electric power by mixing fresh and salt water in the hydroelectric pile, Nature 174 (1954) 660, https://doi.org/10.1038/174660a0.
- [8] D.A. Vermaas, M. Saakes, K. Nijmeijer, Power generation using profiled membranes in reverse electrodialysis, J. Membr. Sci. 385–386 (2011) 234–242, https://doi.org/10.1016/j.memsci.2011.09.043.
- [9] M. Turek, B. Bandura, Renewable energy by reverse electrodialysis, Desalination 205 (2007) 67–74, https://doi.org/10.1016/j.desal.2006.04.041.
- [10] M. Olsson, G.L. Wick, J.D. Isaacs, Salinity gradient power: utilizing vapor pressure differences, Science 206 (1979) 452–454, https://doi.org/10.1126/ science.206.4417.452.
- [11] D. Brogioli, Extracting renewable energy from a salinity difference using a capacitor, Phys. Rev. Lett. 103 (2009) 058501, n/a.
- [12] I. Atlas, G.Z. Ramon, Periodic energy conversion in an electric-double-layer capacitor, J. Colloid Interface Sci. 530 (2018) 675–685, https://doi.org/10.1016/ j.icis.2018.06.034.
- [13] F. La Mantia, M. Pasta, H.D. Deshazer, B.E. Logan, Y. Cui, Batteries for efficient energy extraction from a water salinity difference, Nano Lett. 11 (2011) 1810–1813, https://doi.org/10.1021/nl200500s.
- [14] C. Costentin, T.R. Porter, J.-M. Savéant, How do pseudocapacitors store energy? Theoretical analysis and experimental illustration, ACS Appl. Mater. Interfaces 9 (2017) 8649–8658, https://doi.org/10.1021/acsami.6b14100.
- [15] Y. Jiao, C. Yang, Y. Kang, Energy conversion from salinity gradients by forward osmosis-electrokinetics, J. Phys. Chem. C 118 (2014) 10574–10583, https://doi. org/10.1021/ip412032b.
- [16] A. Siria, P. Poncharal, A.-L. Biance, R. Fulcrand, X. Blase, S.T. Purcell, L. Bocquet, Giant osmotic energy conversion measured in a single transmembrane boron nitride nanotube, Nature 494 (2013) 455–458, https://doi.org/10.1038/ nature11876.
- [17] J. Ji, Q. Kang, Y. Zhou, Y. Feng, X. Chen, J. Yuan, W. Guo, Y. Wei, L. Jiang, Osmotic power generation with positively and negatively charged 2D nanofluidic membrane pairs, Adv. Funct. Mater. 27 (2017), 1603623, https://doi.org/ 10.1002/adfm.201603623.
- [18] W. Ouyang, W. Wang, H. Zhang, W. Wu, Z. Li, Nanofluidic crystal: a facile, high-efficiency and high-power-density scaling up scheme for energy harvesting based on nanofluidic reverse electrodialysis, Nanotechnology 24 (2013), 345401, https://doi.org/10.1088/0957-4484/24/34/345401.
- [19] Z. Wang, L. Wang, M. Elimelech, Viability of harvesting salinity gradient (blue) energy by nanopore-based osmotic power generation, Engineering (2021), https://doi.org/10.1016/j.eng.2021.02.016.
- [20] Y. Jiao, Y. Kang, C. Yang, Osmosis and its applications, in: D. Li (Ed.), Encyclopedia of Microfluidics and Nanofluidics, SpringerNew York, New York, NY, 2015, pp. 2622–2633.
- [21] S. Marbach, L. Bocquet, Osmosis, from molecular insights to large-scale applications, Chem. Soc. Rev. 48 (2019) 3102–3144, https://doi.org/10.1039/ c8cs00420i.
- [22] A.G. Fane, A grand challenge for membrane desalination: more water, less carbon, Desalination 426 (2018) 155–163, https://doi.org/10.1016/j. desal.2017.11.002.
- [23] M.A. Abdelkareem, M. El Haj Assad, E.T. Sayed, B. Soudan, Recent progress in the use of renewable energy sources to power water desalination plants, Desalination 435 (2018) 97–113, https://doi.org/10.1016/j.desal.2017.11.018.

- [24] S. Lee, J. Choi, Y.-G. Park, H. Shon, C.H. Ahn, S.-H. Kim, Hybrid desalination processes for beneficial use of reverse osmosis brine: current status and future prospects, Desalination 454 (2019) 104–111, https://doi.org/10.1016/j. desal.2018.02.002
- [25] J. Bundschuh, M. Kaczmarczyk, N. Ghaffour, B. Tomaszewska, State-of-the-art of renewable energy sources used in water desalination: present and future prospects, Desalination 508 (2021), 115035, https://doi.org/10.1016/j. desal.2021.115035.
- [26] R.R. Gonzales, A. Abdel-Wahab, S. Adham, D.S. Han, S. Phuntsho, W. Suwaileh, N. Hilal, H.K. Shon, Salinity gradient energy generation by pressure retarded osmosis: a review, Desalination 500 (2021), 114841, https://doi.org/10.1016/j. desal 2020 114841
- [27] S. Sarp, Z. Li, J. Saththasivam, Pressure retarded osmosis (PRO): past experiences, current developments, and future prospects, Desalination 389 (2016) 2–14, https://doi.org/10.1016/j.desal.2015.12.008.
- [28] R.A. Tufa, S. Pawlowski, J. Veerman, K. Bouzek, E. Fontananova, G. di Profio, S. Velizarov, J. Goulão Crespo, K. Nijmeijer, E. Curcio, Progress and prospects in reverse electrodialysis for salinity gradient energy conversion and storage, Appl. Energ. 225 (2018) 290–331, https://doi.org/10.1016/j.apenergy.2018.04.111.
- [29] A. Seppälä, M.J. Lampinen, Thermodynamic optimizing of pressure-retarded osmosis power generation systems, J. Membr. Sci. 161 (1999) 115–138, https://doi.org/10.1016/S0376-7388(99)00108-8.
- [30] H. Strathmann, Ion-Exchange Membrane Separation Processes, Elsevier, Burlington, 2004.
- [31] K.L. Lee, R.W. Baker, H.K. Lonsdale, Membranes for power-generation by pressure-retarded osmosis, J. Membr. Sci. 8 (1981) 141–171, https://doi.org/ 10.1016/S0376-7388(00)82088-8.
- [32] S. Loeb, G.D. Mehta, A two-coefficient water transport equation for pressure-retarded osmosis, J. Membr. Sci. 4 (1978) 351–362, https://doi.org/10.1016/S0376-7388(00)83313-X.
- [33] K. Touati, F. Tadeo, Green energy generation by pressure retarded osmosis: state of the art and technical advancement—review, Int.J.Green Energy 14 (2017) 337–360, https://doi.org/10.1080/15435075.2016.1255633.
- [34] S. Lee, C. Boo, M. Elimelech, S. Hong, Comparison of fouling behavior in forward osmosis (FO) and reverse osmosis (RO), J. Membr. Sci. 365 (2010) 34–39, https://doi.org/10.1016/j.memsci.2010.08.036.
- [35] S.C. Chen, C.F. Wan, T.-S. Chung, Enhanced fouling by inorganic and organic foulants on pressure retarded osmosis (PRO) hollow fiber membranes under high pressures, J. Membr. Sci. 479 (2015) 190–203, https://doi.org/10.1016/j. memsci.2015.01.037.
- [36] J. Kim, B. Kim, D. Inhyuk Kim, S. Hong, Evaluation of apparent membrane performance parameters in pressure retarded osmosis processes under varying draw pressures and with draw solutions containing organics, J. Membr. Sci. 493 (2015) 636-644. https://doi.org/10.1016/j.memsci.2015.07.035.
- [37] X. Li, T. Cai, G.L. Amy, T.-S. Chung, Cleaning strategies and membrane flux recovery on anti-fouling membranes for pressure retarded osmosis, J. Membr. Sci. 522 (2017) 116–123, https://doi.org/10.1016/j.memsci.2016.09.016.
- [38] J.H. Jhaveri, Z.V.P. Murthy, A comprehensive review on anti-fouling nanocomposite membranes for pressure driven membrane separation processes, Desalination 379 (2016) 137–154, https://doi.org/10.1016/j.desal.2015.11.009.
- [39] P.-F. Sun, T.-S. Kim, H.-S. Kim, S.-Y. Ham, Y. Jang, Y.-G. Park, C.Y. Tang, H.-D. Park, Improved anti-biofouling performance of pressure retarded osmosis (PRO) by dosing with chlorhexidine gluconate, Desalination 481 (2020), 114376, https://doi.org/10.1016/j.desal.2020.114376.
- [40] J. Zhang, W.L.C. Loong, S. Chou, C. Tang, R. Wang, A.G. Fane, Membrane biofouling and scaling in forward osmosis membrane bioreactor, J. Membr. Sci. 403 (2012) 8–14, https://doi.org/10.1016/j.memsci.2012.01.032.
- [41] Y. Liu, B. Mi, Effects of organic macromolecular conditioning on gypsum scaling of forward osmosis membranes, J. Membr. Sci. 450 (2014) 153–161, https://doi. org/10.1016/j.memsci.2013.09.001.
- [42] S.L. Plata, A.E. Childress, Limiting power density in pressure-retarded osmosis: observation and implications, Desalination 467 (2019) 51–56, https://doi.org/ 10.1016/j.desal.2019.05.013.
- [43] E. Nagy, A general, resistance-in-series, salt- and water flux models for forward osmosis and pressure-retarded osmosis for energy generation, J. Membr. Sci. 460 (2014) 71–81, https://doi.org/10.1016/j.memsci.2014.02.021.
- [44] S. Zhao, L. Zou, Relating solution physicochemical properties to internal concentration polarization in forward osmosis, J. Membr. Sci. 379 (2011) 459–467, https://doi.org/10.1016/j.memsci.2011.06.021.
- [45] A. D'Haese, E.E. Licon Bernal, A. Yaroshchuk, Model of forward osmosis through composite/asymmetric membranes: effects of support inhomogeneity and solution non-ideality, J. Membr. Sci. 602 (2020), 117950, https://doi.org/ 10.1016/j.memsci.2020.117950.
- [46] M. Arjmandi, M. Peyravi, A. Altaee, A. Arjmandi, M. Pourafshari Chenar, M. Jahanshahi, E. Binaeian, A state-of-the-art protocol to minimize the internal concentration polarization in forward osmosis membranes, Desalination 480 (2020), 114355, https://doi.org/10.1016/j.desal.2020.114355.
- [47] T.P.N. Nguyen, B.-M. Jun, H.G. Park, S.-W. Han, Y.-K. Kim, H.K. Lee, Y.-N. Kwon, Concentration polarization effect and preferable membrane configuration at pressure-retarded osmosis operation, Desalination 389 (2016) 58–67, https://doi. org/10.1016/j.desal.2016.02.028.
- [48] D.I. Kim, J. Kim, S. Hong, Changing membrane orientation in pressure retarded osmosis for sustainable power generation with low fouling, Desalination 389 (2016) 197–206, https://doi.org/10.1016/j.desal.2016.01.008.

[49] G.D. Mehta, S. Loeb, Internal polarization in the porous substructure of a semipermeable membrane under pressure-retarded osmosis, J. Membr. Sci. 4 (1978) 261–265, https://doi.org/10.1016/S0376-7388(00)83301-3.

- [50] N.Y. Yip, A. Tiraferri, W.A. Phillip, J.D. Schiffman, L.A. Hoover, Y.C. Kim, M. Elimelech, Thin-film composite pressure retarded osmosis membranes for sustainable power generation from salinity gradients, Environ Sci Technol. 45 (2011) 4360–4369, https://doi.org/10.1021/es104325z.
- [51] N.Y. Yip, M. Elimelech, Performance limiting effects in power generation from salinity gradients by pressure retarded osmosis, Environ. Sci. Technol. 45 (2011) 10273–10282, https://doi.org/10.1021/es203197e.
- [52] A.P. Straub, A. Deshmukh, M. Elimelech, Pressure-retarded osmosis for power generation from salinity gradients: is it viable? Energy Environ.Sci. 9 (2016) 31–48, https://doi.org/10.1039/c5ee02985f.
- [53] S. Loeb, F. Van Hessen, D. Shahaf, Production of energy from concentrated brines by pressure-retarded osmosis: II. Experimental results and projected energy costs, J. Membr. Sci. 1 (1976) 249–269, https://doi.org/10.1016/s0376-7388(00) 82271-1.
- [54] A. Achilli, A.E. Childress, Pressure retarded osmosis: from the vision of Sidney Loeb to the first prototype installation — review, Desalination 261 (2010) 205–211, https://doi.org/10.1016/j.desal.2010.06.017.
- [55] H.H.G. Jellinek, H. Masuda, Osmo-power.Theory and performance of an osmo-power pilot plant, Ocean Eng. 8 (1981) 103–128, https://doi.org/10.1016/0029-8018(81)90022-6.
- [56] K. Gerstandt, K.V. Peinemann, S.E. Skilhagen, T. Thorsen, T. Holt, Membrane processes in energy supply for an osmotic power plant, Desalination 224 (2008) 64–70, https://doi.org/10.1016/j.desal.2007.02.080.
- [57] A. Achilli, T.Y. Cath, A.E. Childress, Power generation with pressure retarded osmosis: an experimental and theoretical investigation, J. Membr. Sci. 343 (2009) 42–52, https://doi.org/10.1016/j.memsci.2009.07.006.
- [58] S. Chou, R. Wang, L. Shi, Q. She, C. Tang, A.G. Fane, Thin-film composite hollow fiber membranes for pressure retarded osmosis (PRO) process with high power density, J. Membr. Sci. 389 (2012) 25–33, https://doi.org/10.1016/j. memsci.2011.10.002.
- [59] Y.C. Kim, Y. Kim, D. Oh, K.H. Lee, Experimental investigation of a spiral-wound pressure-retarded osmosis membrane module for osmotic power generation, Environ. Sci. Technol. 47 (2013) 2966–2973, https://doi.org/10.1021/ es304060d.
- [60] X. Li, T.-S. Chung, Thin-film composite P84 co-polyimide hollow fiber membranes for osmotic power generation, Appl.Energ. 114 (2014) 600–610, https://doi.org/ 10.1016/j.apenergy.2013.10.037.
- [61] M. Higa, D. Shigefuji, M. Shibuya, S. Izumikawa, Y. Ikebe, M. Yasukawa, N. Endo, A. Tanioka, Experimental study of a hollow fiber membrane module in pressure-retarded osmosis: module performance comparison with volumetric-based power outputs, Desalination 420 (2017) 45–53, https://doi.org/10.1016/j.desal.2017.06.015.
- [62] Y. Li, S. Qi, Y. Wang, L. Setiawan, R. Wang, Modification of thin film composite hollow fiber membranes for osmotic energy generation with low organic fouling tendency, Desalination 424 (2017) 131–139, https://doi.org/10.1016/j. desal.2017.10.005.
- [63] M. Sharma, P. Mondal, A. Chakraborty, J. Kuttippurath, M. Purkait, Effect of different molecular weight polyethylene glycol on flat sheet cellulose acetate membranes for evaluating power density performance in pressure retarded osmosis study, J.Water Process Eng. 30 (2019), https://doi.org/10.1016/j. jwpe.2018.05.011.
- [64] S.J. Moon, S.M. Lee, J.H. Kim, S.H. Park, H.H. Wang, J.H. Kim, Y.M. Lee, A highly robust and water permeable thin film composite membranes for pressure retarded osmosis generating 26 W·m—2 at 21 bar, Desalination 483 (2020), 114409, https://doi.org/10.1016/j.desal.2020.114409.
- [65] K.C. Hon, C. Zhao, C. Yang, C.L. Seow, A method of producing electrokinetic power through forward osmosis, Appl. Phys. Lett. 101 (2012) 143902, https://doi.org/10.1063/1.4756903, n/a.
- [66] R.J. Hunter, Zeta Potential in Colloid Science: Principles and Applications, Academic Press, London; New York, 1981.
- [67] D.H. Everett, Basic Principles of Colloid Science, Royal Society of Chemistry, London, 1988.
- [68] C.C. Chang, R.J. Yang, Electrokinetic energy conversion in micrometer-length nanofluidic channels, Microfluid. Nanofluid. 9 (2009) 225–241, https://doi.org/ 10.1007/s10404-009-0538-y.
- [69] F.H.J. van der Heyden, D.J. Bonthuis, D. Stein, C. Meyer, C. Dekker, Power generation by pressure-driven transport of ions in nanofluidic channels, Nano Lett. 7 (2007) 1022–1025, https://doi.org/10.1021/nl070194h.
- [70] H. Daiguji, P. Yang, A.J. Szeri, A. Majumdar, Electrochemomechanical energy conversion in nanofluidic channels, Nano Lett. 4 (2004) 2315–2321, https://doi. org/10.1021/nl0489945.
- [71] M. Wang, Q. Kang, Electrochemomechanical energy conversion efficiency in silica nanochannels, Microfluid. Nanofluid. 9 (2010) 181–190, https://doi.org/ 10.1007/s10404-009-0530-6.
- [72] R. Chein, C. Liao, H. Chen, Electrokinetic energy conversion efficiency analysis using nanoscale finite-length surface-charged capillaries, J. Power Sources 187 (2009) 461–470, https://doi.org/10.1016/j.jpowsour.2008.11.010.
- [73] F.H.J. van der Heyden, D.J. Bonthuis, D. Stein, C. Meyer, C. Dekker, Electrokinetic energy conversion efficiency in nanofluidic channels, Nano Lett. 6 (2006) 2232–2237, https://doi.org/10.1021/nl0615241.
- [74] L. Joly, C. Ybert, E. Trizac, L. Bocquet, Liquid friction on charged surfaces: from hydrodynamic slippage to electrokinetics, J. Chem. Phys. 125 (2006) 204716, https://doi.org/10.1063/1.2397677, n/a.

- [75] C.I. Bouzigues, P. Tabeling, L. Bocquet, Nanofluidics in the debye layer at hydrophilic and hydrophobic surfaces, Phys. Rev. Lett. 101 (2008) 114503, https://doi.org/10.1103/PhysRevLett.101.114503, n/a.
- [76] D. Einzel, P. Panzer, M. Liu, Boundary condition for fluid flow: curved or rough surfaces, Phys. Rev. Lett. 64 (1990) 2269–2272, https://doi.org/10.1103/ PhysRevLett.64.2269.
- [77] L. Joly, C. Ybert, E. Trizac, L. Bocquet, Hydrodynamics within the electric double layer on slipping surfaces, Phys. Rev. Lett. 93 (2004) 257805, https://doi.org/ 10.1103/PhysRevLett.93.257805, n/a.
- [78] Y. Jiao, C. Yang, Y. Kang, K.C. Hon, Enhancement of electrokinetic power generation by surface treatment on a porous glass, in: The 3rd International Conference on Informatics, Environment, Energy and Applications (IEEA 2014), Shanghai, China, 2014, pp. 56–60.
- [79] A. Tiraferri, N.Y. Yip, W.A. Phillip, J.D. Schiffman, M. Elimelech, Relating performance of thin-film composite forward osmosis membranes to support layer formation and structure, J. Membr. Sci. 367 (2011) 340–352, https://doi.org/ 10.1016/i.memsci.2010.11.014.
- [80] N.Y. Yip, A. Tiraferri, W.A. Phillip, J.D. Schiffman, M. Elimelech, High performance thin-film composite forward osmosis membrane, Environ Sci Technol. 44 (2010) 3812–3818, https://doi.org/10.1021/Es1002555.
- [81] R. Wang, L. Shi, C.Y. Tang, S. Chou, C. Qiu, A.G. Fane, Characterization of novel forward osmosis hollow fiber membranes, J. Membr. Sci. 355 (2010) 158–167, https://doi.org/10.1016/j.memsci.2010.03.017.
- [82] S.J. Kwon, K. Park, D.Y. Kim, M. Zhan, S. Hong, J.-H. Lee, High-performance and durable pressure retarded osmosis membranes fabricated using hydrophilized polyethylene separators, J. Membr. Sci. 619 (2021), 118796, https://doi.org/ 10.1016/j.memsci.2020.118796.
- [83] R.R. Gonzales, A. Abdel-Wahab, D.S. Han, H. Matsuyama, S. Phuntsho, H.K. Shon, Control of the antagonistic effects of heat-assisted chlorine oxidative degradation on pressure retarded osmosis thin film composite membrane surface, J. Membr. Sci. 636 (2021), 119567, https://doi.org/10.1016/j.memsci.2021.119567.
- [84] Y. Hartanto, M. Corvilain, H. Mariën, J. Janssen, I.F.J. Vankelecom, Interfacial polymerization of thin-film composite forward osmosis membranes using ionic liquids as organic reagent phase, J. Membr. Sci. 601 (2020), 117869, https://doi. org/10.1016/j.memsci.2020.117869.
- [85] Z. Alihemati, S.A. Hashemifard, T. Matsuura, A.F. Ismail, N. Hilal, Current status and challenges of fabricating thin film composite forward osmosis membrane: a comprehensive roadmap, Desalination 491 (2020), 114557, https://doi.org/ 10.1016/i.desal.2020.114557.
- [86] T.P.N. Nguyen, E.-T. Yun, I.-C. Kim, Y.-N. Kwon, Preparation of cellulose triacetate/cellulose acetate (CTA/CA)-based membranes for forward osmosis, J. Membr. Sci. 433 (2013) 49–59, https://doi.org/10.1016/j. memsci.2013.01.027.
- [87] Z. Wu, P. Ji, B. Wang, N. Sheng, M. Zhang, S. Chen, H. Wang, Oppositely charged aligned bacterial cellulose biofilm with nanofluidic channels for osmotic energy harvesting, Nano Energy 80 (2021), 105554, https://doi.org/10.1016/j. nanoen.2020.105554.
- [88] Y. Wu, W. Xin, X.-Y. Kong, J. Chen, Y. Qian, Y. Sun, X. Zhao, W. Chen, L. Jiang, L. Wen, Enhanced ion transport by graphene oxide/cellulose nanofibers assembled membranes for high-performance osmotic energy harvesting, Mater. Horiz. (2020), https://doi.org/10.1039/D0MH00979B.
- [89] B.S. Lalia, V. Kochkodan, R. Hashaikeh, N. Hilal, A review on membrane fabrication: structure, properties and performance relationship, Desalination 326 (2013) 77–95, https://doi.org/10.1016/j.desal.2013.06.016.
- [90] W. Gai, D.L. Zhao, T.-S. Chung, Novel thin film composite hollow fiber membranes incorporated with carbon quantum dots for osmotic power generation, J. Membr. Sci. 551 (2018) 94–102, https://doi.org/10.1016/j. memsci. 2018.01.034.
- [91] M. Asadollahi, D. Bastani, S.A. Musavi, Enhancement of surface properties and performance of reverse osmosis membranes after surface modification: a review, Desalination 420 (2017) 330–383, https://doi.org/10.1016/j.desal.2017.05.027.
- [92] S.-P. Sun, T.-S. Chung, Outer-selective pressure-retarded osmosis hollow fiber membranes from vacuum-assisted interfacial polymerization for osmotic power generation, Environ Sci Technol. 47 (2013) 13167–13174, https://doi.org/ 10.1021/es403270n.
- [93] Z.L. Cheng, X. Li, Y.D. Liu, T.-S. Chung, Robust outer-selective thin-film composite polyethersulfone hollow fiber membranes with low reverse salt flux for renewable salinity-gradient energy generation, J. Membr. Sci. 506 (2016) 119–129, https://doi.org/10.1016/j.memsci.2015.12.060.
- [94] S. Lin, A.P. Straub, M. Elimelech, Thermodynamic limits of extractable energy by pressure retarded osmosis, energy and environmental, Science 7 (2014) 2706–2714, https://doi.org/10.1039/c4ee01020e.
- [95] A. Altaee, J. Zhou, A. Alhathal Alanezi, G. Zaragoza, Pressure retarded osmosis process for power generation: feasibility, energy balance and controlling parameters, Appl.Energ. 206 (2017) 303–311, https://doi.org/10.1016/j. appergry 2017 08 195
- [96] S.E. Skilhagen, J.E. Dugstad, R.J. Aaberg, Osmotic power power production based on the osmotic pressure difference between waters with varying salt gradients, Desalination 220 (2008) 476–482, https://doi.org/10.1016/j. desal.2007.02.045.
- [97] K.S. Pitzer, J.C. Peiper, R.H. Busey, Thermodynamic properties of aqueous sodium chloride solutions, J. Phys. Chem. Ref. Data 13 (1984) 1–102, https://doi. org/10.1063/1.555709.
- [98] F. Helfer, C. Lemckert, The power of salinity gradients: an Australian example, Renew. Sustain. Energy Rev. 50 (2015) 1–16, https://doi.org/10.1016/j. rser.2015.04.188.

- [99] M.L. Stone, C. Rae, F.F. Stewart, A.D. Wilson, Switchable polarity solvents as draw solutes for forward osmosis, Desalination 312 (2013) 124–129, https://doi. org/10.1016/j.desal.2012.07.034.
- [100] N. Bajraktari, C. Hélix-Nielsen, H.T. Madsen, Pressure retarded osmosis from hypersaline sources — a review, Desalination 413 (2017) 65–85, https://doi.org/ 10.1016/j.desal.2017.02.017.
- [101] E.S.H. Lee, J.Y. Xiong, G. Han, C.F. Wan, Q.Y. Chong, T.-S. Chung, A pilot study on pressure retarded osmosis operation and effective cleaning strategies, Desalination 420 (2017) 273–282, https://doi.org/10.1016/j.desal.2017.08.004.
- [102] F. Helfer, C. Lemckert, Y.G. Anissimov, Osmotic power with pressure retarded osmosis: theory, performance and trends – a review, J. Membr. Sci. 453 (2014) 337–358, https://doi.org/10.1016/j.memsci.2013.10.053.
- [103] Q. She, X. Jin, C.Y. Tang, Osmotic power production from salinity gradient resource by pressure retarded osmosis: effects of operating conditions and reverse solute diffusion, J. Membr. Sci. 401–402 (2012) 262–273, https://doi.org/ 10.1016/j.memsci.2012.02.014.
- [104] Y.C. Kim, M. Elimelech, Adverse impact of feed channel spacers on the performance of pressure retarded osmosis, Environ. Sci. Technol. 46 (2012) 4673–4681, https://doi.org/10.1021/es3002597.
- [105] S. Chou, R. Wang, A.G. Fane, Robust and high performance hollow fiber membranes for energy harvesting from salinity gradients by pressure retarded osmosis, J. Membr. Sci. 448 (2013) 44–54, https://doi.org/10.1016/j. memsci.2013.07.063.
- [106] X. Song, Z. Liu, D.D. Sun, Energy recovery from concentrated seawater brine by thin-film nanofiber composite pressure retarded osmosis membranes with high power density, <sb:contribution><sb:title>Energy Environ. </sb:title></sb: contribution><sb:host><sb:issue></sb:eries><sb:title>Sci.</sb:title></sb: series></sb:issue></sb:host> 6 (2013) 1199–1210, https://doi.org/10.1039/ c3ee23349a.
- [107] Y.C. Kim, M. Elimelech, Potential of osmotic power generation by pressure retarded osmosis using seawater as feed solution: analysis and experiments, J. Membr. Sci. 429 (2013) 330–337, https://doi.org/10.1016/j. memsci.2012.11.039.
- [108] G. Han, Q. Ge, T.-S. Chung, Conceptual demonstration of novel closed-loop pressure retarded osmosis process for sustainable osmotic energy generation, Appl.Energ. 132 (2014) 383–393, https://doi.org/10.1016/j. apenergy.2014.07.029.
- [109] F.-J. Fu, S.-P. Sun, S. Zhang, T.-S. Chung, Pressure retarded osmosis dual-layer hollow fiber membranes developed by co-casting method and ammonium persulfate (APS) treatment, J. Membr. Sci. 469 (2014) 488–498, https://doi.org/ 10.1016/j.memsci.2014.05.063.
- [110] S. Zhang, P. Sukitpaneenit, T.-S. Chung, Design of robust hollow fiber membranes with high power density for osmotic energy production, Chem. Eng. J. 241 (2014) 457–465, https://doi.org/10.1016/j.cej.2013.10.063.
- [111] A.P. Straub, N.Y. Yip, M. Elimelech, Raising the bar: increased hydraulic pressure allows unprecedented high power densities in pressure-retarded osmosis, Environ.Sci.Technol.Lett. 1 (2014) 55–59, https://doi.org/10.1021/ez400117d.
- [112] C.F. Wan, T.-S. Chung, Osmotic power generation by pressure retarded osmosis using seawater brine as the draw solution and wastewater retentate as the feed, J. Membr. Sci. 479 (2015) 148–158, https://doi.org/10.1016/j. memsci.2014.12.036.
- [113] D.D. Anastasio, J.T. Arena, E.A. Cole, J.R. McCutcheon, Impact of temperature on power density in closed-loop pressure retarded osmosis for grid storage, J. Membr. Sci. 479 (2015) 240–245, https://doi.org/10.1016/j. memsci.2014.12.046.
- [114] Y.C. Kim, J.H. Lee, S.-J. Park, Novel crossflow membrane cell with asymmetric channels: design and pressure-retarded osmosis performance test, J. Membr. Sci. 476 (2015) 76–86, https://doi.org/10.1016/j.memsci.2014.11.018.
- [115] Y. Li, R. Wang, S. Qi, C. Tang, Structural stability and mass transfer properties of pressure retarded osmosis (PRO) membrane under high operating pressures, J. Membr. Sci. 488 (2015) 143–153, https://doi.org/10.1016/j. memsci.2015.04.030.
- [116] D. Zhao, G. Qiu, X. Li, C. Wan, K. Lu, T.-S. Chung, Zwitterions coated hollow fiber membranes with enhanced antifouling properties for osmotic power generation from municipal wastewater, Water Res. 104 (2016) 389–396, https://doi.org/ 10.1016/j.watres.2016.08.045.
- [117] J. Wei, Y. Li, L. Setiawan, R. Wang, Influence of macromolecular additive on reinforced flat-sheet thin film composite pressure-retarded osmosis membranes, J. Membr. Sci. 511 (2016) 54–64, https://doi.org/10.1016/j. memsci.2016.03.046.
- [118] K.L. Hickenbottom, J. Vanneste, M. Elimelech, T.Y. Cath, Assessing the current state of commercially available membranes and spacers for energy production with pressure retarded osmosis, Desalination 389 (2016) 108–118, https://doi. org/10.1016/j.desal.2015.09.029.
- [119] B. Al-Anzi, A. Thomas, J. Fernandes, Lab scale assessment of power generation using pressure retarded osmosis from wastewater treatment plants in the state of Kuwait, Desalination 396 (2016) 57–69, https://doi.org/10.1016/j. doi:10.1016/00.005
- [120] M. Kurihara, H. Sakai, A. Tanioka, H. Tomioka, Role of pressure-retarded osmosis (PRO) in the mega-ton water project, Desalin. Water Treat. 57 (2016) 26518–26528, https://doi.org/10.1080/19443994.2016.1168582.
- [121] C.F. Wan, B. Li, T. Yang, T.-S. Chung, Design and fabrication of inner-selective thin-film composite (TFC) hollow fiber modules for pressure retarded osmosis (PRO), Sep. Purif. Technol. 172 (2017) 32–42, https://doi.org/10.1016/j. seppur.2016.08.001.

- [122] Q.A. Khasawneh, B. Tashtoush, A. Nawafleh, B. Kan'an, Techno-economic feasibility study of a hypersaline pressure-retarded osmosis power plants: Dead sea-red Sea conveyor, Energies. 11 (2018), https://doi.org/10.3390/ en.1113118.
- [123] E. Marin-Coria, R. Silva, C. Enriquez, M.L. Martínez, E. Mendoza, Environmental assessment of the impacts and benefits of a salinity gradient energy pilot plant, Energies. 14 (2021) 3252, https://doi.org/10.3390/en14113252.
- [124] Y. Xu, X. Peng, C.Y. Tang, Q.S. Fu, S. Nie, Effect of draw solution concentration and operating conditions on forward osmosis and pressure retarded osmosis performance in a spiral wound module, J. Membr. Sci. 348 (2010) 298–309, https://doi.org/10.1016/j.memsci.2009.11.013.
- [125] W. He, Y. Wang, M.H. Shaheed, Energy and thermodynamic analysis of power generation using a natural salinity gradient based pressure retarded osmosis process, Desalination 350 (2014) 86–94, https://doi.org/10.1016/j. desal.2014.07.015.
- [126] A. Altaee, G. Zaragoza, E. Drioli, J. Zhou, Evaluation the potential and energy efficiency of dual stage pressure retarded osmosis process, Appl.Energ. 199 (2017) 359–369, https://doi.org/10.1016/j.apenergy.2017.05.031.
- [127] W. He, Y. Wang, M.H. Shaheed, Enhanced energy generation and membrane performance by two-stage pressure retarded osmosis (PRO), Desalination 359 (2015) 186–199, https://doi.org/10.1016/j.desal.2014.12.014.
- [128] A. Altaee, N. Hilal, Design optimization of high performance dual stage pressure retarded osmosis, Desalination 355 (2015) 217–224, https://doi.org/10.1016/j. desal.2014.11.002.
- [129] J. Kim, J. Lee, J.H. Kim, Overview of pressure-retarded osmosis (PRO) process and hybrid application to sea water reverse osmosis process, Desalin. Water Treat. 43 (2012) 193–200, https://doi.org/10.1080/19443994.2012.672170.
- [130] R.L. McGinnis, J.R. McCutcheon, M. Elimelech, A novel ammonia-carbon dioxide osmotic heat engine for power generation, J. Membr. Sci. 305 (2007) 13–19, https://doi.org/10.1016/j.memsci.2007.08.027.
- [131] P. Chelme-Ayala, D.W. Smith, M.G. El-Din, Membrane concentrate management options: a comprehensive critical review, J. Environ. Eng. Sci. 8 (2013) 326–339, https://doi.org/10.1680/jees.2013.0033.
- [132] L.F. Greenlee, D.F. Lawler, B.D. Freeman, B. Marrot, P. Moulin, Reverse osmosis desalination: water sources, technology, and today's challenges, Water Res. 43 (2009) 2317–2348, https://doi.org/10.1016/j.watres.2009.03.010.
- [133] A. Ravizky, N. Nadav, Salt production by the evaporation of SWRO brine in Eilat: a success story, Desalination 205 (2007) 374–379, https://doi.org/10.1016/j. desal.2006.03.559.
- [134] G. Han, S. Zhang, X. Li, T.-S. Chung, Progress in pressure retarded osmosis (PRO) membranes for osmotic power generation, Prog. Polym. Sci. 51 (2015) 1–27, https://doi.org/10.1016/j.progpolymsci.2015.04.005.
- [135] S. Adhikary, M.S. Islam, K. Touati, S. Sultana, A.S. Ramamurthy, M.S. Rahaman, Increased power density with low salt flux using organic draw solutions for pressure-retarded osmosis at elevated temperatures, Desalination 484 (2020), 114420. https://doi.org/10.1016/j.desal.2020.114420.
- [136] K. Touati, C. Hänel, F. Tadeo, T. Schiestel, Effect of the feed and draw solution temperatures on PRO performance: theoretical and experimental study, Desalination 365 (2015) 182–195, https://doi.org/10.1016/j.desal.2015.02.016.
- [137] B. Abdelkader, M.H. Sharqawy, Temperature effects and entropy generation of pressure retarded osmosis process, Entropy 21 (2019) 1158, https://doi.org/ 10.3390/e21121158.
- [138] K. Touati, F. Tadeo, C. Hänel, T. Schiestel, Effect of the operating temperature on hydrodynamics and membrane parameters in pressure retarded osmosis, Desalin. Water Treat. 57 (2016) 10477–10489, https://doi.org/10.1080/ 19443994.2015.1039600.
- [139] G. O'Toole, L. Jones, C. Coutinho, C. Hayes, M. Napoles, A. Achilli, River-to-sea pressure retarded osmosis: resource utilization in a full-scale facility, Desalination 389 (2016) 39–51, https://doi.org/10.1016/j.desal.2016.01.012.
- [140] S. Loeb, Large-scale power production by pressure-retarded osmosis, using river water and sea water passing through spiral modules, Desalination 143 (2002) 115–122, https://doi.org/10.1016/S0011-9164(02)00233-3.
- [141] D.-K. Kim, A. Majumdar, S.J. Kim, Electrokinetic flow meter, Sensors Actuators A Phys. 136 (2007) 80–89, https://doi.org/10.1016/j.sna.2006.10.022.
- [142] A. Mansouri, S. Bhattacharjee, L. Kostiuk, High-power electrokinetic energy conversion in a glass microchannel array, Lab Chip 12 (2012) 4033–4036, https://doi.org/10.1039/c2lc40525c.
- [143] A. Mansouri, S. Bhattacharjee, L.W. Kostiuk, Electrokinetic energy conversion by microchannel array: electrical analogy, experiments, and electrode polarization, J. Phys. Chem. C 118 (2014) 24310–24324, https://doi.org/10.1021/jp507790y.
- [144] S.H. Kwak, S.-R. Kwon, S. Baek, S.-M. Lim, Y.-C. Joo, T.D. Chung, Densely charged polyelectrolyte-stuffed nanochannel arrays for power generation from salinity gradient, Sci. Rep.-Uk. 6 (2016) doi:Artn 2641610.1038/Srep26416.
- [145] L. Zaraska, M. Jaskuła, G.D. Sulka, Porous anodic alumina layers with modulated pore diameters formed by sequential anodizing in different electrolytes, Mater. Lett. 171 (2016) 315–318, https://doi.org/10.1016/j.matlet.2016.02.113.
- [146] A. Belwalkar, E. Grasing, W.H. Van Geertruyden, Z. Huang, W.Z. Misiolek, Effect of processing parameters on pore structure and thickness of anodic aluminum oxide (AAO) tubular membranes, J. Membr. Sci. 319 (2008) 192–198, https:// doi.org/10.1016/j.memsci.2008.03.044.
- [147] A. Yaroshchuk, T. Luxbacher, Interpretation of electrokinetic measurements with porous films: role of electric conductance and streaming current within porous structure, Langmuir 26 (2010) 10882–10889, https://doi.org/10.1021/ la1007772.

- [148] S. Saksena, A.L. Zydney, Pore size distribution effects on electrokinetic phenomena in semipermeable membranes, J. Membr. Sci. 105 (1995) 203–215, https://doi.org/10.1016/0376-7388(95)00060-P.
- [149] E.E. Meyer, K.J. Rosenberg, J. Israelachvili, Recent progress in understanding hydrophobic interactions, Proc. Natl. Acad. Sci. U. S. A. 103 (2006) 15739–15746, https://doi.org/10.1073/pnas.0606422103.
- [150] N.V. Churaev, J. Ralston, I.P. Sergeeva, V.D. Sobolev, Electrokinetic properties of methylated quartz capillaries, Adv. Colloid Interf. Sci. 96 (2002) 265–278, https://doi.org/10.1016/s0001-8686(01)00084-7.
- [151] H.A. Stone, A.D. Stroock, A. Ajdari, Engineering flows in small devices: microfluidics toward a lab-on-a-Chip, Annu. Rev. Fluid Mech. 36 (2004) 381–411, https://doi.org/10.1146/annurev.fluid.36.050802.122124.
- [152] C. Davidson, X. Xuan, Electrokinetic energy conversion in slip nanochannels, J. Power Sources 179 (2008) 297–300, https://doi.org/10.1016/j. jpowsour.2007.12.050.
- [153] Y. Ren, D. Stein, Slip-enhanced electrokinetic energy conversion in nanofluidic channels, Nanotechnology 19 (2008) doi:Artn 19570710.1088/0957-4484/19/ 19/195707.
- [154] J. Eijkel, Liquid slip in micro- and nanofluidics: recent research and its possible implications, Lab Chip 7 (2007) 299–301, https://doi.org/10.1039/b700364c.
- [155] M. Rezaei, A.R. Azimian, A.R. Pishevar, Surface charge-dependent hydrodynamic properties of an electroosmotic slip flow, Phys. Chem. Chem. Phys. 20 (2018) 30365–30375, https://doi.org/10.1039/c8cp06408c.
- [156] H. Nabeshi, T. Yoshikawa, A. Arimori, T. Yoshida, S. Tochigi, T. Hirai, T. Akase, K. Nagano, Y. Abe, H. Kamada, S.-I. Tsunoda, N. Itoh, Y. Yoshioka, Y. Tsutsumi, Effect of surface properties of silica nanoparticles on their cytotoxicity and cellular distribution in murine macrophages, Nanoscale Res. Lett. 6 (2011) 93, https://doi.org/10.1186/1556-276X-6-93.
- [157] Y. Shin, D. Lee, K. Lee, K.H. Ahn, B. Kim, Surface properties of silica nanoparticles modified with polymers for polymer nanocomposite applications, J. Ind. Eng. Chem. 14 (2008) 515–519, https://doi.org/10.1016/j.jiec.2008.02.002.
- [158] Y. Xie, J.D. Sherwood, L. Shui, A. van den Berg, J.C.T. Eijkel, Strong enhancement of streaming current power by application of two phase flow, Lab Chip 11 (2011) 4006–4011, https://doi.org/10.1039/c1lc20423h.
- [159] C.L.A. Berli, Output pressure and efficiency of electrokinetic pumping of non-Newtonian fluids, Microfluid. Nanofluid. 8 (2010) 197–207, https://doi.org/ 10.1007/s10404-009-0455-0.
- [160] R.B. Bird, Dynamics of Polymeric Liquids, 2nd ed., Wiley, New York, 1987.
- [161] H. Daiguji, Y. Oka, T. Adachi, K. Shirono, Theoretical study on the efficiency of nanofluidic batteries, Electrochem. Commun. 8 (2006) 1796–1800, https://doi. org/10.1016/j.elecom.2006.08.003.
- [162] X. Xuan, D. Li, Thermodynamic analysis of electrokinetic energy conversion, J. Power Sources 156 (2006) 677–684, https://doi.org/10.1016/j. ipowsour.2005.05.057.
- [163] R. Chein, K. Tsai, L. Yeh, Analysis of effect of electrolyte types on electrokinetic energy conversion in nanoscale capillaries, Electrophoresis 31 (2010) 535–545, https://doi.org/10.1002/elps.200900409.
- [164] T. Nguyen, Y. Xie, L.J. de Vreede, A. van den Berg, J.C.T. Eijkel, Highly enhanced energy conversion from the streaming current by polymer addition, Lab Chip 13 (2013) 3210–3216, https://doi.org/10.1039/c3lc41232f.
- [165] B. Fan, P.R. Bandaru, Tensorial modulation of electrokinetic streaming potentials on air and liquid filled surfaces, Langmuir 35 (2019) 14812–14817, https://doi. org/10.1021/acs.langmuir.9b02841.
- [166] B. Fan, P.R. Bandaru, Modulation of the streaming potential and slip characteristics in electrolyte flow over liquid-filled surfaces, Langmuir 35 (2019) 6203–6210, https://doi.org/10.1021/acs.langmuir.9b00704.
- [167] J. Harting, C. Kunert, J. Hyväluoma, Lattice boltzmann simulations in microfluidics: probing the no-slip boundary condition in hydrophobic, rough, and surface nanobubble laden microchannels, Microfluid. Nanofluid. 8 (2009) 1, https://doi.org/10.1007/s10404-009-0506-6.
- [168] J. Zhang, K. Zhan, S. Wang, X. Hou, Soft interface design for electrokinetic energy conversion, Soft Matter 16 (2020) 2915–2927, https://doi.org/10.1039/ C9SM02506E.
- [169] G. Han, J. Zuo, C. Wan, T.-S. Chung, Hybrid pressure retarded osmosis-membrane distillation (PRO-MD) process for osmotic power and clean water generation, Environ.Sci. Water Res.Technol. 1 (2015) 507, https://doi.org/10.1039/ C5FW00127G.
- [170] R.A. Tufa, E. Curcio, E. Brauns, W. van Baak, E. Fontananova, G. Di Profio, Membrane distillation and reverse electrodialysis for near-zero liquid discharge and low energy seawater desalination, J. Membr. Sci. 496 (2015) 325–333, https://doi.org/10.1016/j.memsci.2015.09.008.
- [171] B.J. Feinberg, G.Z. Ramon, E.M.V. Hoek, Thermodynamic analysis of osmotic energy recovery at a reverse osmosis desalination plant, Environ. Sci. Technol. 47 (2013) 2982–2989, https://doi.org/10.1021/es304224b.
- [172] J.L. Prante, J.A. Ruskowitz, A.E. Childress, A. Achilli, RO-PRO desalination: an integrated low-energy approach to seawater desalination, Appl.Energ. 120 (2014) 104–114, https://doi.org/10.1016/j.apenergy.2014.01.013.
- [173] D.I. Kim, J. Kim, H.K. Shon, S. Hong, Pressure retarded osmosis (PRO) for integrating seawater desalination and wastewater reclamation: energy consumption and fouling, J. Membr. Sci. 483 (2015) 34–41, https://doi.org/ 10.1016/j.memsci.2015.02.025.
- [174] K. Kwon, J. Han, B.H. Park, Y. Shin, D. Kim, Brine recovery using reverse electrodialysis in membrane-based desalination processes, Desalination 362 (2015) 1–10, https://doi.org/10.1016/j.desal.2015.01.047.
- [175] T.T.D. Tran, K. Park, A.D. Smith, System scaling approach and thermoeconomic analysis of a pressure retarded osmosis system for power production with

- hypersaline draw solution: a Great Salt Lake case study, Energy 126 (2017) 97–111, https://doi.org/10.1016/j.energy.2017.03.002.
- [176] S. Gormly, J. Herron, M. Flynn, M. Hammoudeh, H. Shaw, Forward osmosis for applications in sustainable energy development, Desalin. Water Treat. 27 (2011) 327–333, https://doi.org/10.5004/dwt.2011.2596.
- [177] C. Lee, S.H. Chae, E. Yang, S. Kim, J.H. Kim, I.S. Kim, A comprehensive review of the feasibility of pressure retarded osmosis: recent technological advances and industrial efforts towards commercialization, Desalination 491 (2020), 114501, https://doi.org/10.1016/j.desal.2020.114501.
- [178] K. Touati, H.S. Usman, C.N. Mulligan, M.S. Rahaman, Energetic and economic feasibility of a combined membrane-based process for sustainable water and energy systems, Appl. Energ. 264 (2020), 114699, https://doi.org/10.1016/j. apenergy.2020.114699.
- [179] A. Al-Othman, N.N. Darwish, M. Qasim, M. Tawalbeh, N.A. Darwish, N. Hilal, Nuclear desalination: a state-of-the-art review, Desalination 457 (2019) 39–61, https://doi.org/10.1016/j.desal.2019.01.002.
- [180] M. Tawalbeh, A. Al-Othman, K. Singh, I. Douba, D. Kabakebji, M. Alkasrawi, Microbial desalination cells for water purification and power generation: a critical review, Energy 209 (2020), 118493, https://doi.org/10.1016/j. energy.2020.118493.
- [181] G.A. Bemporad, The use of pressure-retarded osmosis for increasing the solar pond efficiency, Sol. Energy 48 (1992) 375–379, https://doi.org/10.1016/0038-092X(92)90046-D.
- [182] J. Benjamin, M.E. Arias, Q. Zhang, A techno-economic process model for pressure retarded osmosis based energy recovery in desalination plants, Desalination 476 (2020), 114218, https://doi.org/10.1016/j.desal.2019.114218.
- [183] A. Zapata-Sierra, M. Cascajares, A. Alcayde, F. Manzano-Agugliaro, Worldwide research trends on desalination, Desalination 519 (2022), 115305, https://doi. org/10.1016/j.desal.2021.115305.
- [184] C. Fritzmann, J. Löwenberg, T. Wintgens, T. Melin, State-of-the-art of reverse osmosis desalination, Desalination 216 (2007) 1–76, https://doi.org/10.1016/j. desal.2006.12.009.

- [185] H. Shemer, D. Hasson, R. Semiat, State-of-the-art review on post-treatment technologies, Desalination 356 (2015) 285–293, https://doi.org/10.1016/j. desal.2014.09.035.
- [186] Z.M. Binger, G. O'Toole, A. Achilli, Evidence of solution-diffusion-with-defects in an engineering-scale pressure retarded osmosis system, J. Membr. Sci. 625 (2021), 119135, https://doi.org/10.1016/j.memsci.2021.119135.
- [187] S. Lee, T.-S. Park, Y.-G. Park, W.-I. Lee, S.-H. Kim, Toward scale-up of seawater reverse osmosis (SWRO) – pressure retarded osmosis (PRO) hybrid system: a case study of a 240 m3/day pilot plant, Desalination 491 (2020), 114429, https://doi. org/10.1016/j.desal.2020.114429.
- [188] H. Manzoor, M.A. Selam, S. Adham, H.K. Shon, M. Castier, A. Abdel-Wahab, Energy recovery modeling of pressure-retarded osmosis systems with membrane modules compatible with high salinity draw streams, Desalination 493 (2020), 114624, https://doi.org/10.1016/j.desal.2020.114624.
- [189] A. Altaee, A. Sharif, Pressure retarded osmosis: advancement in the process applications for power generation and desalination, Desalination 356 (2015) 31–46, https://doi.org/10.1016/j.desal.2014.09.028.
- [190] J. Kim, M. Park, S.A. Snyder, J.H. Kim, Reverse osmosis (RO) and pressure retarded osmosis (PRO) hybrid processes: model-based scenario study, Desalination 322 (2013) 121–130, https://doi.org/10.1016/j.desal.2013.05.010.
- [191] A. Altaee, G. Zaragoza, A. Sharif, Pressure retarded osmosis for power generation and seawater desalination: performance analysis, Desalination 344 (2014) 108–115, https://doi.org/10.1016/j.desal.2014.03.022.
- [192] S. Senthil, S. Senthilmurugan, Reverse osmosis-pressure retarded osmosis hybrid system: modelling, simulation and optimization, Desalination 389 (2016) 78–97, https://doi.org/10.1016/j.desal.2016.01.027.
- [193] C.F. Wan, T.-S. Chung, Energy recovery by pressure retarded osmosis (PRO) in SWRO-PRO integrated processes, Appl.Energ. 162 (2016) 687–698, https://doi. org/10.1016/j.apenergy.2015.10.067.
- [194] S. Pennathur, J.C.T. Eijkel, A. van den Berg, Energy conversion in microsystems: is there a role for micro/nanofluidics? Lab Chip 7 (2007) 1234–1237, https://doi. org/10.1039/b712893m.